

Dual Protein Farnesyltransferase–Geranylgeranyltransferase-I Inhibitors as Potential Cancer Chemotherapeutic Agents

S. Jane deSolms,[†] Terrence M. Ciccarone,[†] Suzanne C. MacTough,[†] Anthony W. Shaw,[†] Carolyn A. Buser,[‡] Michelle Ellis-Hutchings,[‡] Christine Fernandes,[‡] Kelly A. Hamilton,[‡] Hans E. Huber,[‡] Nancy E. Kohl,[‡] Robert B. Lobell,[‡] Ronald G. Robinson,[‡] Nancy N. Tsou,[#] Eileen S. Walsh,[‡] Samuel L. Graham,^{*,†} Lorena S. Beese,[‡] and Jeffrey S. Taylor[‡]

Departments of Medicinal Chemistry and Cancer Research, Merck Research Laboratories, West Point, Pennsylvania 19486, Department of Molecular Design & Diversity, Merck Research Laboratories, Rahway, New Jersey 07065, and Department of Biochemistry, Duke University Medical Center, Durham, North Carolina 27710

Received December 27, 2002

A series of novel diaryl ether lactams have been identified as very potent dual inhibitors of protein farnesyltransferase (FTase) and protein geranylgeranyltransferase I (GGTase-I), enzymes involved in the prenylation of Ras. The structure of the complex formed between one of these compounds and FTase has been determined by X-ray crystallography. These compounds are the first reported to inhibit the prenylation of the important oncogene Ki-Ras4B *in vivo*. Unfortunately, doses sufficient to achieve this endpoint were rapidly lethal.

Introduction

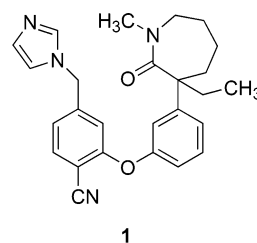
The ras oncogene product Ras p21 plays an important role in controlling cell proliferation. Mutations in Ras can lead to unregulated cell growth and are implicated in 20–30% of all human tumors.¹ Protein farnesyltransferase (FTase), a zinc metalloenzyme, catalyzes the S-farnesylation of a cysteine residue in the C-terminal tetrapeptide (CAAX) sequence of Ras. This prenylation is an essential first step in the localization of Ras to the plasma membrane, whereupon further post-translational modifications enable signal transduction and, in the case of mutant Ras, uncontrolled cell growth.

Considerable effort has focused on the development of selective FTase inhibitors as potential cancer chemotherapeutics.² Early studies with these agents demonstrated effective reversion of the transformed phenotype of cells bearing an activating mutation in the Harvey isoform of Ras (H-Ras). Altered cellular morphology and growth inhibition occurred at compound doses that coincided with blockade of H-Ras farnesylation. Inhibition of H-Ras farnesylation was achieved without affecting the prenylation of geranylgeranylated proteins such as Rap1A.³

The most frequently mutated form of Ras in human cancers, however, is Ki-Ras4B (K-Ras). Ordinarily, K-Ras appears to be almost exclusively farnesylated by FTase *in vivo*. However, inhibition of FTase does not lead to the accumulation of unprenylated K-Ras. Instead, K-Ras becomes geranylgeranylated by the closely related enzyme protein geranylgeranyltransferase-I (GGTase-I) in a reaction that is only a few-fold less efficient than farnesylation. Geranylgeranylated K-Ras appears to be fully competent for transducing growth

factor signals.^{4,5} Thus, inhibition of both FTase and GGTase-I would be required to inhibit K-Ras-dependent biology and a single molecule with dual inhibitory properties could potentially be a useful chemotherapeutic agent.

Previously⁶ we have demonstrated that imidazole-methyl diaryl ethers are potent inhibitors of FTase with a spectrum of activity vs GGTase-I. In particular, the racemic compound **1** exhibited excellent activity in both



enzyme assays (FTase IC₅₀ = 2.9 nM, GGTase-I IC₅₀ = 7.1 nM). In this paper, we describe modifications of **1** that provided extremely potent dual FTase/GGTase-I inhibitors that have good activity in cell culture and can inhibit the prenylation of K-Ras *in vivo*.

Chemistry

The syntheses of **1** and several analogues thereof are described in Schemes 1–8. A convergent strategy was used in which two comparably sized fragments were joined by a nucleophilic aromatic substitution reaction that formed the ether linkage.

The phenolic components for the syntheses were prepared (Scheme 1) following a procedure described by White⁷ for the synthesis of the analgesic meptazinol. Thus, the enolate derived from *N*-methylazepinone **3a** was treated with the *m*-methoxybenzyl precursor **2** to afford anisole **4a**. Generation of the enolate from **4a** and reaction with several alkylating agents provided a family of anisoles **4b–h**. These compounds were resolved by chiral-phase chromatography and demethylated with boron tribromide to obtain the corresponding

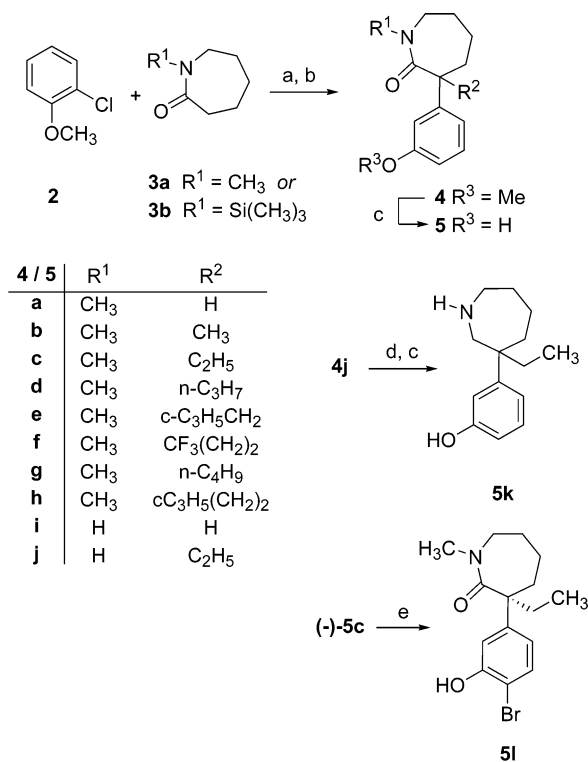
* To whom correspondence should be addressed. Address: Department of Medicinal Chemistry, Merck Research Laboratories, WP14-2, P.O. Box 4, West Point, PA 19486. Phone: (215) 652-6979. Fax: (215) 652-7310. E-mail: sam_graham@merck.com.

[†] Department of Medicinal Chemistry, Merck Research Laboratories.

[‡] Department of Cancer Research, Merck Research Laboratories.

[#] Department of Molecular Design and Diversity, Merck Research Laboratories.

[‡] Duke University Medical Center.

Scheme 1. Phenolic Intermediates^a

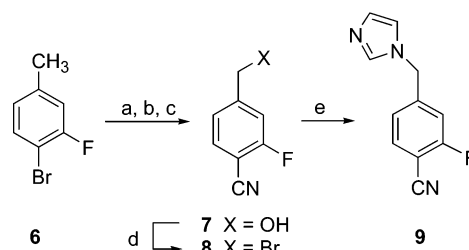
^a Reagents: (a) LiTMP; (b) R²X, LiTMP; (c) BBr₃, CH₂Cl₂; (d) LiAlH₄, THF; (e) NBS, DMF.

phenols **5a–h**. The absolute stereochemistry of (–)-**5c** was determined to be *S* by X-ray crystallographic analysis of the derived bromide **5l** (see Supporting Information). The stereochemistry ascribed to the other resolved phenols was assumed from their optical rotation and their relative mobility on chiral-phase chromatography and was supported by consistent patterns of enzyme-inhibitory activity that were observed for the diastereomers of the final compounds.

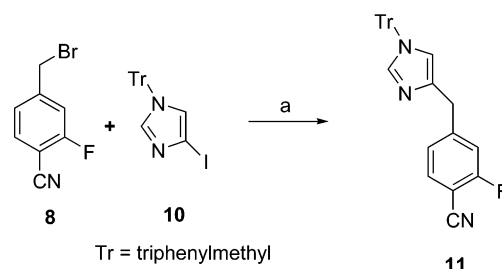
To prepare compounds without substitution on the azepinone nitrogen, the benzyne chemistry and alkylation were carried out using *N*-trimethylsilylazepinone **3b**, again following White's precedent. The silyl group cleaved spontaneously upon workup to provide, after demethylation, the phenols **5i** and **5j**. Reduction of the amide carbonyl of **4j** with LiAlH₄ and phenol demethylation gave the amine **5k**.

2-Fluoro-4-imidazolylmethylbenzonitrile **9**⁸ was prepared from 4-bromo-3-fluorotoluene via 4-bromomethyl-2-fluorobenzonitrile⁹ (**8**) by a straightforward reaction sequence, as described in Scheme 2. Since the benzylic linkage to N-1 of the imidazole ring of **1** was perceived as a potential site for metabolic *N*-dealkylation, the regioisomeric fragment **11**, with the benzyl group appended to C-5 of the imidazole, was prepared by Suzuki coupling of **8** with 4-iodo-1-tritylimidazole¹⁰ (**10**).

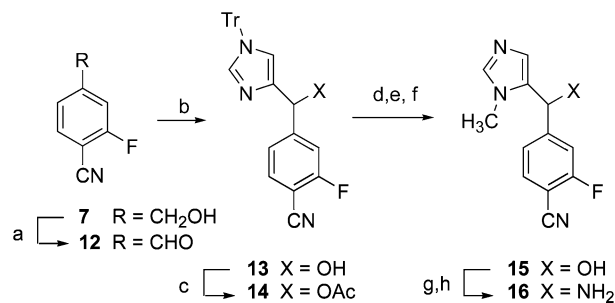
Analogues of **11** with a higher degree of functionalization at the benzylic linker were prepared as shown in Scheme 4. Swern oxidation of alcohol **7** gave the aldehyde **12**.⁶ Addition of the Grignard reagent derived from **10–12** led to alcohol **13**. After conversion of **13** to the corresponding acetate, the imidazole nitrogen was alkylated with dimethyl sulfate and the trityl group was removed by methanolysis of the intermediate imidazolium salt. The acetate was hydrolyzed to give alcohol

Scheme 2. Preparation of *N*-Substituted Imidazole Fragment^a

^a Reagents: (a) KMnO₄, H₂O/pyridine; (b) borane–THF, THF; (c) Zn(CN)₂, Pd[PPh₃]₄, DMF; (d) CBr₄, PPh₃, CH₂Cl₂; (e) imidazole, DMF.

Scheme 3. Preparation of *C*-Substituted Imidazole Fragment^a

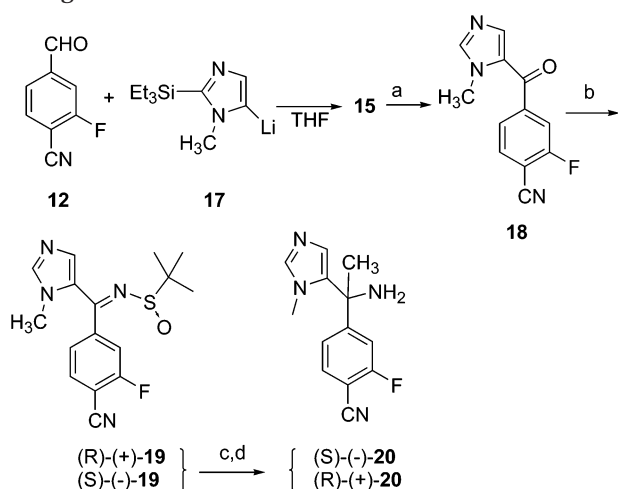
^a Reagents: (a) Zn, NiCl₂(PPh₃)₂, BrCH₂CH₂Br, THF.

Scheme 4. Synthesis of Functionalized Analogues of **11**^a

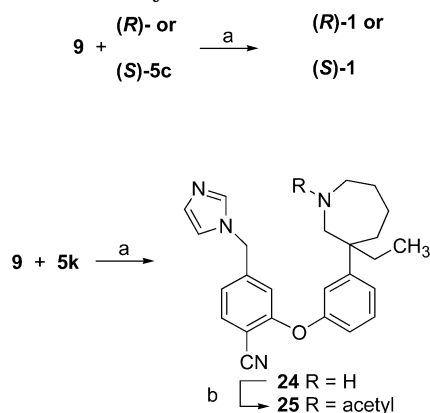
^a Reagents: (a) pyridine–SO₃, DMSO, CH₂Cl₂; (b) **10**, EtMgBr, CH₂Cl₂; (c) Ac₂O, pyr, DMF; (d) (CH₃)₂SO₄, EtOAc; (e) CH₃OH; (f) NaOH, THF; (g) SOCl₂; (h) NH₃, CHCl₃.

15. Treatment of **15** sequentially with thionyl chloride and ammonia gave the amine **16**.

An efficient, asymmetric synthesis of the aminated fluorobenzonitrile intermediate **20** is shown in Scheme 5. Reaction of aldehyde **12** with lithiated imidazole **17**¹¹ provided direct access to the alcohol **15**. To obtain enantiomerically enriched **20**, the use of diaryl ketones in Ellman's¹² method for the asymmetric preparation of amines was explored. Thus, the chiral sulfinylimines (*R*)- and (*S*)-**19** were prepared. Methyl Grignard reagent addition to (*R*)-**19** gave a 4:1 mixture of diastereomeric sulfinamides from which the major diastereomer could be purified by recrystallization. Cleavage of the sulfinyl group gave the levorotatory amine (–)-**20**. On the basis of crystallographic data described below, the levorotatory isomer can be assigned the *S* stereochemistry. Using methyl lithium instead of the Grignard gave the opposite sense of stereoselection, with the same degree of selectivity, leading to (+)-**20**. Since this was the first example of diastereoselective transformation of a diaryl ketone using Ellman's method, the scope of this reaction was further explored, as described elsewhere.¹³

Scheme 5. Alternative, Asymmetric Synthesis of Analogues of **16**^a

^a Reagents: (a) MnO_2 , CH_2Cl_2 ; (b) (*R*)- or (*S*)-*tert*-BuSONH₂, $\text{Ti}(\text{OEt})_4$, THF; (c) MeMgBr , THF, 0 °C; (d) MeOH, HCl.

Scheme 6. Phenol Arylation with Benzonitrile **9**^a

^a Reagents: (a) $\text{KF}/\text{Al}_2\text{O}_3$, 18-crown-6, CH_3CH ; (b) CH_3COCl , Et_3N , CH_2Cl_2 .

The enantiomers of **1** were prepared (Scheme 6) by reaction of each of the enantiomers of phenol **5c** with benzonitrile **9** in the presence of $\text{KF}/\text{alumina}$. Similarly, reaction of **9** with racemic phenols **5a**, **5i**, and **5j** gave compounds **21–23**. Also, azepane **24**, derived from **5k**, was further transformed by acetylation to **25**. Compounds prepared from **9** are shown in Table 1.

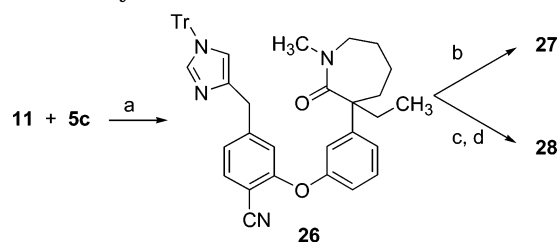
Arylation of phenol **5c** with the tritylated imidazole **11** also occurred readily using $\text{KF}/\text{alumina}$ to provide intermediate **26** (Scheme 7). Detritylation of **26** with $\text{TFA}/\text{Et}_3\text{SiH}$ gave **27** (Table 2). Alternatively, methylation of **26** and solvolysis of the resulting imidazolium salt gave the N-1 methyl derivative **28**.

Ether formation between the benzyl alcohol **15** and racemic **5c** gave the expected ether **29**, which could be further transformed to the amine **30** (Scheme 8). An attempt at the direct formation of **30** by reaction of the benzylic amine **16** with **5c** led primarily to ketone **31**, an autoxidation product. This unexpected product was converted via Grignard reaction to the tertiary alcohol **32** from which the amine **33** was prepared. Initially, chiral phase chromatography was used to separate the four stereoisomers of **33**. Subsequently the more efficient assembly of these compounds was attained by coupling enantiomerically enriched fragments **5c** and

Table 1. Azebinone Modifications of **1**

compd	R ¹	R ²	X	IC ₅₀ , nM (<i>n</i>) ^a	
				FTase	GGTase-I
(<i>RS</i>)- 1	CH ₃	C ₂ H ₅	O	3.0 (2)	7.2 ± 0.6 (6)
(<i>R</i>)- 1	CH ₃	C ₂ H ₅	O	5.3	25 (2)
(<i>S</i>)- 1	CH ₃	C ₂ H ₅	O	1.4	5.8 (2)
(<i>RS</i>)- 21	CH ₃	H	O	61	560 ± 60 (4)
(<i>RS</i>)- 22	H	H	O	41	1200 (2)
(<i>RS</i>)- 23	H	C ₂ H ₅	O	1.3	20 (2)
(<i>RS</i>)- 24	H	C ₂ H ₅	H, H	100	280 (2)
(<i>RS</i>)- 25	C(C=O)CH ₃	C ₂ H ₅	H, H	1.9	8.9

^a *n* = number of determinations. For assays with *n* > 2, data are reported as the mean ± SEM. If *n* is unreported, the data represent a single determination. Standard errors in the enzyme assays were typically less than ±50% of the mean.

Scheme 7. Synthesis of **27** and **28**^a

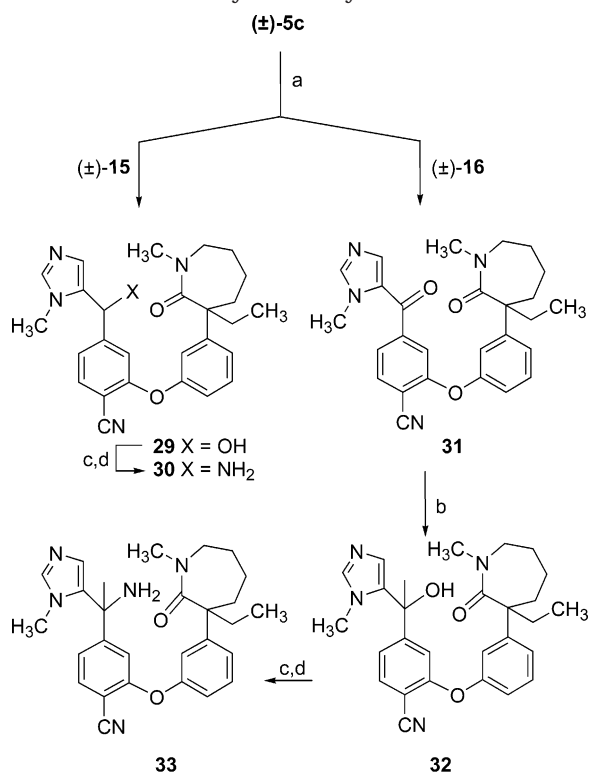
^a Reagents: (a) $\text{KF}/\text{Al}_2\text{O}_3$, 18-crown-6, CH_3CH ; (b) Et_3SiH , TFA ; (c) $(\text{CH}_3\text{O})_2\text{SO}_2$, EtOAc ; (d) MeOH.

Table 2. 5-Substituted Imidazoles

compd	R ¹	R ²	R ³	IC ₅₀ , nM (<i>n</i>) ^a	
				FTase	GGTase-I
27	H	H	H	13	12
28	CH ₃	H	H	0.6	10 ± 1 (4)
29	CH ₃	OH	H	2.0	17 (2)
30	CH ₃	NH ₂	H	0.19	8 (2)
31	CH ₃	=O		1800	10000
32	CH ₃	OH	CH ₃	1.2	13 ± 5 (3)
33	CH ₃	NH ₂	CH ₃	0.38	5.1 ± 2.0 (3)

^a *n* = number of determinations. For assays with *n* > 2, data are reported as the mean ± SEM. If *n* is unreported, the data represent a single experiment. Standard errors for enzyme assays were typically less than ±50% of the mean. Compounds were tested as mixtures of all possible diastereomers.

20 under the standard $\text{KF}/\text{alumina}$ conditions. Tables 2 and 3 summarize the compounds prepared using these methods. Diaryl ether formation under the conditions described above using enantiomerically enriched **20** with a variety of resolved phenols **5** gave the compounds shown in Table 4. Only the most potent diastereomer, resulting in each case from reaction of (*S*)-(-)-**20** with (-)-**5**,¹⁴ is reported in the Table.

Scheme 8. Phenol Arylation: Syntheses of **29–33**^a

^a Reagents: (a) KF/Al₂O₃, 18-crown-6, CH₃CN; (b) MeMgBr, THF; (c) SOCl₂; (d) NH₃, CHCl₃.

Structure–Activity Relationships

All compounds were assayed for their ability to inhibit FTase and GGTase-I in vitro. As previously described, compound **1** was a dual FTase–GGTase-I inhibitor of good potency (Table 1). Resolution of this compound revealed that the *S* enantiomer of **1** is a more potent inhibitor of both FTase and GGTase-I in vitro (FTase IC₅₀ = 1.4 nM, GGTase-I IC₅₀ = 5.8 nM) than (*R*)-**1** (FTase IC₅₀ = 5.3 nM, GGTase-I IC₅₀ = 25 nM). Compound (*R,S*)-**21**, which lacks the ethyl substituent on the azepinone in **1**, is 20- and 80-fold less potent than (*R,S*)-**1** as an FTI and GGTI, respectively. Compounds **22** and **23** demonstrate that the lactam *N*-methyl substituent in **1** is not important for FTase activity, although it may contribute slightly to GGTase-I activity. The importance of the azepinone ethyl group to the intrinsic potency of this family of inhibitors is underscored by the reduced potency of **22** in comparison to **23**.

Converting the amide group in **23** to an amine in **24** resulted in a 100-fold loss of potency against FTase and a more modest 14-fold reduction in GGTase-I inhibitory activity. Most of this activity can be restored by acetylating the lactam nitrogen to give **25**.

The data in Table 2 show the impact of changing the position of substitution on the imidazole group from N-1 to C-5 in the context of the ethyl-substituted azepinone. Compound (*R,S*)-**27**, a monosubstituted imidazole, was 2- to 4-fold less potent than (*R,S*)-**1** as an FTI and GGTI. Methylating N-1 of the imidazole gave a compound ((*R,S*)-**28**) that was equipotent to (*R,S*)-**1**. Hydroxylation and amination of the benzylic carbon of **28** gave compounds **29** and **30** (each prepared as a mixture of four stereoisomers). Although the hydroxyl substituent di-

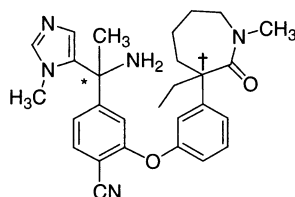
minished potency slightly, the amino group in **30** appeared to improve affinity for FTase. However, compound **30** was highly susceptible to air oxidation, affording ketone **31**. This ketone was several-hundred-fold less active than **28** as an FTI or GGTI.

Encouraged by the potency of **29** and **30** but concerned about their chemical and metabolic stability, we replaced the remaining benzylic hydrogen with a methyl group to provide compounds **32** and **33** (Table 2), initially prepared and evaluated as mixtures of four diastereomers. The hydroxy compound (**32**) was comparable to **29** in potency but remained slightly less active than the unsubstituted compound **28** as an inhibitor of prenyltransferases. The methylated amino compound **33** was similar in activity to **30**, but again, the amino group appeared to contribute slightly greater affinity for FTase and GGTase-I compared to **28**. The properties of each of the four diastereomers of **33** (**33a–d**) are shown in Table 3. The stereoisomers vary in FTase inhibitory potency over a 100-fold range, with the stereoisomer resulting from the coupling of (*S*)-**5c** and (–)-**20** being an extremely potent inhibitor (60 pM). GGTase-I activity was somewhat less sensitive to the stereostructure of these inhibitors. The crystallographic data presented below for **33a** revealed that the levorotatory fragment (–)-**20** has the *S* configuration.

Table 4 illustrates the effect of the substituent at the 3-position of the azepinone ring on enzyme inhibition. While all four diastereomers of these compounds were prepared, data are provided only for the most potent isomer, which invariably arose from coupling the levorotatory enantiomers of **5** and **20**. For all isomers of the compounds in Table 4, the same pattern of inhibitory potency as a function of stereochemistry was observed as for the isomers of **33**. Thus, with respect to the optical rotation of the fragments **5** and **20**, the rank order of IC₅₀ was (–)/(–) < (–)/(+) < (+)/(–) < (+)/(+).

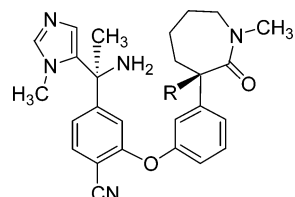
For both enzymes the least potent inhibitor is **34**, which is unsubstituted at the 3-position of the azepinone. While the presence of a non-hydrogen substituent on the azepinone ring is clearly beneficial in this series, a profound relationship between substituent size or hydrophobicity and activity is not obvious. For the majority of substituents we explored, potency varied only 2- to 4-fold.

Structure of an Inhibitor–FTase Complex. A crystal structure of human farnesyltransferase was obtained with compound **33a** bound in the active site, and the data are represented graphically in Figure 1. The compound, clearly possessing the *S,S* stereochemistry, occupies the space where the peptide substrate is normally bound,¹⁵ while the binding of FPP is unaffected by the inhibitor. The most striking features of the complex are the direct ligation of the active site zinc atom by N-3 of the imidazole and the close packing of the isoprenoid and cyanophenyl hydrophobic surfaces. The location of the cyano group in the vicinity of Arg202β may provide an additional favorable polar interaction within the complex. The central phenyl group of **33a** makes hydrophobic interactions with Trp102, Trp106, Trp303, and Tyr361 of the β subunit, as well as with the tail of the isoprenoid chain. The aliphatic portion of the azepinone ring resides in a predominantly hydrophobic pocket bounded by Ala151,

Table 3. Diastereomers of **33**

compd	*	†	IC ₅₀ , ^a nM		protein processing inhibition EC ₅₀ , nM (<i>n</i>) ^b		
			FTase	GGTase-I	HDJ2	Rap1a	K-Ras
33a	<i>S</i>	<i>S</i>	0.06	3.6	2.1 ± 0.9 (3)	470 ± 20 (3)	340 ± 50 (3)
33b	<i>S</i>	<i>R</i>	1.5	4.5	11	720	1900
33c	<i>R</i>	<i>S</i>	0.36	13	6	140	230
33d	<i>R</i>	<i>R</i>	7.6	54	120	3200	8000

^a Average of two determinations. ^b Results of a single determination except for **33a**, for which the average of *n* = 3 determinations ± SEM is reported.

Table 4. Effects of Azeponone Substitution on Activity

compd	R	IC ₅₀ , nM (<i>n</i>) ^a		protein processing EC ₅₀ , nM (<i>n</i>) ^b		
		FTase	GGTase-I	HDJ2	Rap1a	K-Ras
34^c	H	11 (1)	92 (2)			
35^d	CH ₃	0.41 (2)	30 (2)	26 (1)	3990 (1)	3730 (1)
36	C ₃ H ₇	0.46 (3)	2.9 (2)	0.9 (2)	220 (2)	100 (2)
37	<i>c</i> -C ₃ H ₅ CH ₂	0.3 (1)	2.1 (2)	1.5 (2)	87 (2)	220 (2)
38	CF ₃ CH ₂ CH ₂	0.19 (2)	2.5 (2)	3.1 (2)	47 (2)	207 ± 65 (4)
39	C ₄ H ₉	0.12 (2)	1.4 (2)	4 (2)	250 (2)	320 (2)
40	<i>c</i> -C ₃ H ₅ CH ₂ CH ₂	0.18 (1)	0.81 (2)	11 (1)	> 1000 (1)	1290 (1)

^a *n* = number of determinations. Standard deviations for enzyme assays were typically ±50% of the mean or less. ^b Average of *n* determinations. Replicate values typically differed less than 2-fold. ^c Assays run with a 1:1 mixture of compounds arising from the asymmetric center on the azeponone ring. ^d Processing assays were performed on a mixture of the four diastereomers of **35**.

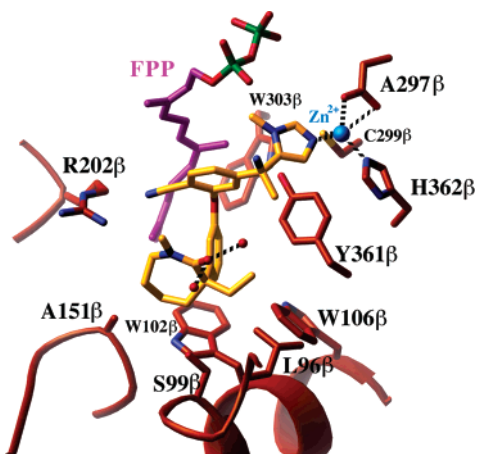


Figure 1. Crystal structure of **33a** (yellow) bound to hFTase. The farnesyl hydrocarbon is shown in magenta. Two crystallographically defined water molecules are shown near the lactam carbonyl.

Trp102, and Ser99 of the β subunit, while the ethyl group lies near Leu96 and Trp106. The lactam carbonyl is solvent-exposed and interacts with a crystallographically well-defined water molecule.

An interesting feature of the structure–activity relationships is the stereoselectivity in the binding of the pairs of amino compounds differing only in configuration

at the carbon bearing the primary amine (e.g., **33a** and **33c**), where the *S* configuration is preferred by 5- to 6-fold. In **33a**, the (presumably protonated) amine is near the phosphate group of FPP, although the distance between the amine and nearest phosphate oxygen (N–O separation of 4.3 Å) is too great to represent a contact ion pair, such as had been observed in an FTase complex with a peptidomimetic inhibitor (N–O separation of 2.7 Å).¹⁵ Well-ordered water molecules capable of mediating a hydrogen-bonding interaction are also absent. However, it remains plausible that a solvent-separated ion pair could contribute to binding, an interaction that would be diminished upon inversion of configuration.

Changing the configuration of the asymmetric center in the azeponone ring has an even larger effect on binding affinity (20- to 25-fold) than is observed for the primary amine-bearing carbon. If one assumes that the ethyl and aryl groups in **33a** and **33b** occupy similar sites in the enzyme, then the azeponone carbonyl, which is exposed to solvent in the complex of **33a**, would project toward Trp102 and Ser99 of the β subunit, while the hydrocarbon segment is removed from its preferred hydrophobic environment to one that is solvent-exposed.

Another interesting aspect of the SAR is the large loss in potency that accrues upon reduction of the lactam of **23** to the amine **24**. As noted above, the lactam carbonyl in the crystal structure does not appear to make any

important interactions with the enzyme but is solvent-exposed, interacting with a nearby water molecule. Perhaps an unfavorable interaction of the protonated amine in the reduction product with Arg202 β (N–N distance of 4.7 Å) or insertion of the methylene group from the former carbonyl into an aqueous environment contributes to the loss of activity. The restoration of activity upon acetylation suggests that the electrostatic interaction may be of greater importance.

Mechanism of Inhibition of GGTase-I

The crystallographic analysis of **33a** in complex with FTase defines the mechanism of inhibition as protein substrate competitive, as is the case for many other cyanobenzylimidazole-containing compounds.¹⁶ For GGTase, we have previously reported that cyanobenzylimidazoles can inhibit GGTase in competition with either peptide or prenyl pyrophosphate substrates.¹⁷ To define the mechanism of inhibition of GGTase-I by these diaryl ethers, the IC₅₀ for inhibition of GGTase-I by six of the compounds in Table 4 was redetermined at three concentrations of GGPP (see Experimental Section). The slopes of the plots of log IC₅₀ vs log [GGPP] for these compounds varied from –0.28 to –0.03, indicating that the compounds are not competitive, and possibly uncompetitive, vs GGPP. Thus, in common with the mechanism of inhibition of FTase, and similar to some of our earlier compounds,¹⁷ inhibition of GGTase by competition with the peptide substrate is highly likely.

Inhibition of Protein Prenylation

We also determined the relationship of intrinsic enzyme inhibitory potency to inhibition of protein prenylation in cultured PSN-1 pancreatic carcinoma cells.¹⁸ As representative intracellular substrates, we used the chaperone protein hDJ as an example of a purely farnesylated substrate and the small GTPase Rap1a as a specifically geranylgeranylated protein. The prenylation state of K-Ras, a substrate for both enzymes, was also evaluated. For the diastereomers of **33**, inhibition of hDJ protein processing was rank-ordered correctly by intrinsic enzyme inhibitory activity (Table 3). However, a quantitative correlation is absent. The relationship between Rap1a processing and in vitro GGTase-I inhibition is less apparent and may be obscured by the relatively small range of GGTase-I inhibitory activities displayed by this set of compounds. The compounds in Table 4 were also evaluated in the processing assays. Since there is significant variation in the chemical constitution of these compounds, it is not surprising that intrinsic enzyme inhibitory potency does not predict potency in the processing assays. In particular, the most hydrophobic compound (**40**) is significantly less potent in cell culture than might have been predicted from its enzyme inhibitory activities. Note that the apparent anomaly in the processing activity of **35** is largely attributable to the use of an equimolar mixture of the four diastereomers of **35** in the processing assay while the enzyme inhibitory data shown refer to the most potent of the diastereomers.

Several of these inhibitors were more efficient inhibitors of K-Ras processing than **33a**. The balance of FTase and GGTase inhibition potency (ratio of EC₅₀ values for Rap1a to HDJ processing is 15) of **38** has been shown¹⁸ to be nearly ideal in that its EC₅₀ for inhibition of K-Ras

processing is not improved in the presence of an excess of either a selective FTase or GGTase inhibitor. In contrast, K-Ras processing inhibition by **33a** (ratio of 224) was markedly enhanced by supplementation with a GGTase inhibitor.

As reported elsewhere,¹⁸ compounds **33a** and **38** were evaluated in mice for antitumor efficacy and toxicity. These studies were challenging because of the poor pharmacokinetic properties of the compounds. They are not orally bioavailable and have rapid apparent clearance in mice. To observe substantial inhibition of K-Ras processing, we resorted to infusion with Alzet osmotic pumps at nominal doses approaching 2000 mpk. Despite the enormous dose, plasma concentrations of about 3–10 μ M were attained. Although at these doses both **33a** and **38** could be shown to inhibit K-Ras prenylation in vivo, attempts to demonstrate antitumor efficacy with these compounds were complicated by severe toxicity. Mice treated for 72 h with doses of inhibitors sufficient to inhibit K-Ras processing showed signs of myelosuppression, became edematous, and suffered 100% mortality. These effects were also seen after treatment with a selective inhibitor of GGTase-I alone. Although an antitumor effect was observed following a 24 h treatment with the dual inhibitors, it was no greater than that achieved with a comparable dose (i.e., equipotent for hDJ processing inhibition) of a pure FTase inhibitor alone. On the basis of these observations, it is unlikely that suppression of K-Ras function by inhibition of its prenylation will be of clinical utility.

It should be noted that the high doses of dual prenyltransferase inhibitors required to inhibit K-Ras prenylation probably suffice to substantially block the prenylation of all substrates of FTase and GGTase-I. As suggested by the studies of Sun et al.,⁴ it remains conceivable that in some settings lower doses of such compounds may have beneficial effects by selective inhibition of the prenylation of a subset of proteins.

Experimental Section

All reagents and starting materials used in the syntheses were purchased from Aldrich, Fisher, Fluka, Sigma, or Lancaster and used without purification. All solvents were purchased from Fisher or Aldrich. Thin-layer chromatography (TLC) was performed on E. Merck 60F-254 (0.25 mm) pre-coated silica gel plates. Visualization of TLC plates was accomplished with UV light and/or phosphomolybdic acid stain.

Flash chromatography was performed on E. Merck silica gel 60 (230–400 mesh) unless otherwise noted. Melting points (mp) were determined on a Thomas-Hoover melting point apparatus and are uncorrected. Preparative HPLC was performed on a Waters DeltaPrep 4000 instrument using either a C-18 Waters PrepPak column or a Vydac column for reverse phase or on Chiral Technologies, Inc. Chiralcel OD or Chiralpak AD columns for chiral normal phase. Proton nuclear magnetic resonance (¹H NMR) spectra were obtained on a Varian XL 300 or 400 spectrometer. Chemical shifts are expressed in ppm relative to tetramethylsilane. Mass spectra were obtained on a VG Micromass MM7035 spectrometer. Elemental analyses were performed on a Perkin-Elmer 2400 analyzer, and results are within $\pm 0.4\%$ of the theoretical value unless indicated otherwise. Optical rotations were measured with a Perkin-Elmer 241 polarimeter.

3-(3-Methoxyphenyl)-1-methylazepan-2-one (4a).⁷ To 1.6 M *n*-BuLi in hexane (187.5 mL, 0.3 mol) at 0 °C was added a solution of 2,2,6,6-tetramethylpiperidine (50.6 mL, 0.3 mol) in anhydrous THF (300 mL) over 5 min under an Ar atmosphere. *N*-Methylazepinone (**3a**, 38.2 g, 0.3 mol) in anhydrous

THF (60 mL) was added. After the reaction mixture was stirred for 10 min, an additional portion of 1.6 M *n*-BuLi in hexane (187.5 mL, 0.3 mol) was added. After the mixture was stirred for 10 min, 2-chloroanisole (**2**, 42.8 g, 0.3 mol) was added. After the mixture was stirred for 30 min, the reaction was quenched with ice-H₂O, and the mixture was stirred for 30 min and concentrated in vacuo. The residue was diluted with EtOAc and washed with 5 N HCl (100 mL) and brine. The organic layer was dried (MgSO₄), concentrated, and purified by silica gel chromatography (0.5% MeOH/CH₂Cl₂) to give 28.35 g (40%) of **4a**. ¹H NMR (CDCl₃): δ 7.20–7.25 (m, 1H), 6.76–6.82 (m, 3H), 3.84–3.88 (m, 1H), 3.80 (s, 3H), 3.64–3.71 (m, 1H), 3.22–3.29 (m, 1H), 3.02 (s, 3H), 1.98–2.06 (m, 3H), 1.77–1.86 (m, 1H), 1.65–1.76 (m, 1H), 1.50–1.59 (m, 1H).

Representative Procedure for the Alkylation of Azepanone 4a: (+)-3-(*R*)-Ethyl-3-(3-methoxyphenyl)-1-methylazepan-2-one ((*R*)-(+)-4c**) and (–)-3-(*S*)-Ethyl-3-(3-methoxyphenyl)-1-methylazepan-2-one ((*S*)-(–)-**4c**).**⁷ To 1.6 M *n*-BuLi in hexane (172 mL, 0.275 mol) at 0 °C was added a solution of 2,2,6,6-tetramethylpiperidine (46.4 mL, 0.275 mol) in anhydrous THF (450 mL) over 15 min under Ar. After the reaction mixture was stirred for 15 min, compound **4a** (31.32 g, 0.134 mol) was added and the mixture was stirred for 1 h at 0 °C. Iodoethane (25.1 g, 0.161 mol) was added in one portion, and the reaction mixture was allowed to warm to room temperature and stirred overnight. The reaction was quenched with ice-H₂O, and the mixture was stirred for 30 min and concentrated in vacuo. The residue was diluted with EtOAc and washed with 5 N HCl (200 mL) and brine. The organic layer was dried (MgSO₄), concentrated, and purified on silica gel (30–50% EtOAc/hexane) to give 10.6 g of **4c** and 14.5 g of recovered **4a** (56% yield based on recovered starting material). Racemic **4c** was separated by HPLC on a ChiralPak AD column eluting with 90:10 hexane/ethanol to give 5.37 g of (*R*)-(+)-**4c**, [α]_D²⁵ +59.8° (c 1, CCl₄), and 5.39 g of (*S*)-(–)-**4c**, [α]_D²⁵ –60.8° (c 1, CCl₄). ¹H NMR (CDCl₃): δ 7.21–7.27 (m, 1H), 6.67–6.78 (m, 3H), 3.80 (s, 3H), 3.05–3.12 (m, 1H), 3.05 (s, 3H), 2.76–2.84 (m, 1H), 2.17–2.24 (m, 1H), 1.82–1.94 (m, 2H), 1.49–1.57 (m, 1H), 1.37–1.68 (m, 1H), 0.75 (t, 3H, *J* = 7 Hz).

3-(3-Methoxyphenyl)azepan-2-one (4i).⁷ Azepinone (10.0 g, 88 mmol), triethylamine (14.8 mL, 106 mmol), and chlorotrimethylsilane (13.5 mL, 106 mmol) were dissolved in 60 mL of toluene and refluxed under argon for 3 h. The mixture was filtered, and the solvent was evaporated to provide *N*-trimethylsilylazepinone (**3b**). The title compound was prepared from this crude intermediate as described for the preparation of **4a**.

2-Ethyl-3-(3-methoxyphenyl)azepan-2-one (4j). To 1.6 M *n*-BuLi in hexane (31.3 mL, 0.05 mol) at 0 °C was added a solution of 2,2,6,6-tetramethylpiperidine (8.43 mL, 0.05 mol) in anhydrous THF (100 mL) over 5 min under an Ar atmosphere. *N*-Trimethylsilylazepinone (**3b**, 9.26 g, 0.05 mol) in anhydrous THF (20 mL) was added. After the reaction mixture was stirred for 10 min, an additional portion of 1.6 M *n*-BuLi in hexane (31.3 mL, 0.05 mol) was added. After the mixture was stirred for 10 min, 2-chloroanisole **2** (6.34 g, 0.05 mol) was added. After the mixture was stirred for 30 min, ethyl iodide (3.90 mL, 48.7 mmol) was added. After 30 min, the reaction was quenched with ice-H₂O, and the mixture was stirred for 30 min and concentrated in vacuo. The residue was diluted with EtOAc and washed with 5 N HCl (100 mL) and brine. The organic layer was dried (MgSO₄), concentrated, and purified using silica gel chromatography (10–15% EtOAc/CH₂Cl₂) to give **4j**.

Representative Procedure for Phenol Demethylation: (–)-3(*S*)-Ethyl-3-(3-hydroxyphenyl)-1-methylazepan-2-one ((*S*)-(–)-5c**).** A 1 M solution of BBr₃ (77.7 mL, 77.7 mmol) in CH₂Cl₂ (80 mL) was added to compound (*S*)-(–)-**4c** (6.04 g, 25.9 mmol) dissolved in anhydrous CH₂Cl₂ (400 mL) at 0 °C under N₂. After 3.5 h, the reaction was quenched with saturated aqueous NaHCO₃ solution and the mixture was extracted with CH₂Cl₂ (3×). The extract was dried (Na₂SO₄) and concentrated to give 4.9 g (76%) of (*S*)-(–)-**5c**, [α]_D²⁵ –43.0° (c 1, EtOH). ¹H NMR (CDCl₃): δ 7.19 (t, 1H, *J* = 7.8 Hz), 6.68–

6.74 (m, 2H), 6.64 (t, 1H, *J* = 2 Hz), 6.35 (br s, 1H), 3.10–3.17 (m, 1H), 3.05 (s, 3H), 2.78–2.85 (m, 1H), 2.17–2.24 (m, 1H), 1.86–2.00 (m, 1H), 1.70–1.86 (m, 4H), 1.51–1.59 (m, 1H), 1.39–1.50 (m, 1H), 0.74 (t, 3H, *J* = 7.3 Hz).

(+)-3(*R*)-Ethyl-3-(3-hydroxyphenyl)-1-methylazepan-2-one (*R*)-(+)-**5c** was prepared in a like manner. [α]_D²⁵ +46.9° (c 1, EtOH).

(3-(3-Ethylazepan-3-yl)phenol (5k). Compound **4j** (1.05 g, 4.24 mmol) in anhydrous THF (4.2 mL) was added to a solution of LiAlH₄ (0.193 g, 5.09 mmol) in anhydrous THF (4.2 mL), and the mixture was refluxed for 24 h. The solution was cooled, quenched with H₂O (0.18 mL), 15% NaOH (0.18 mL), and H₂O (0.54 mL), filtered, and concentrated. The residue was purified using reverse-phase chromatography (95:5 to 5:95 H₂O/CH₃CN with 0.1% TFA, flow = 65 mL/min), converted to its free base using saturated NaHCO₃ solution, extracted with CH₂Cl₂ (3×), and dried (MgSO₄) to give 0.316 g (32%) of **4k**. ¹H NMR (CDCl₃): δ 7.25 (t, 1H, *J* = 8 Hz), 6.90 (d, 1H, *J* = 7.8 Hz), 6.87 (t, 1H, *J* = 2 Hz), 6.73 (dd, 1H, *J* = 2, 8 Hz), 3.81 (s, 3H), 3.23 (d, 1H, *J* = 14.2 Hz), 2.92–2.96 (m, 1H), 2.87 (d, 1H, *J* = 14.2 Hz), 2.74–2.80 (m, 1H), 2.20–2.25 (m, 1H), 1.51–1.76 (m, 7H), 0.60 (t, 3H, *J* = 7.3 Hz).

A 1 M solution of BBr₃ (2.56 mL, 2.56 mmol) in CH₂Cl₂ was added to compound **4k** (0.300 g, 0.128 mmol) dissolved in anhydrous CH₂Cl₂ (10 mL) at –78 °C. After the mixture was stirred for 20 h at room temperature, the reaction was quenched with saturated NaHCO₃ solution and the mixture was extracted with CH₂Cl₂ (3×), dried (MgSO₄), and concentrated to give 0.28 g (100%) of **5k**. ¹H NMR (CDCl₃): δ 7.21 (t, 1H, *J* = 8 Hz), 6.80 (d, 1H, *J* = 8 Hz), 6.78 (s, 1H), 6.70 (d, 1H, *J* = 8.2 Hz), 4.6 (v br s, 2H), 3.46 (d, 1H, *J* = 14.6 Hz), 2.90–2.98 (m, 1H), 2.84 (d, 1H, *J* = 14.2 Hz), 2.78–2.88 (m, 1H), 2.32–2.39 (m, 1H), 1.64–1.80 (m, 3H), 1.50–1.59 (m, 4H), 0.62 (t, 3H, *J* = 7.2 Hz).

(–)-3(*S*)-Ethyl-3-(4-bromo-3-hydroxyphenyl)-1-methylazepan-2-one ((*S*)-(–)-**5l**).

To a solution of (–)-**5c** (0.10 g, 0.404 mmol) in DMF (2 mL) was added dropwise a solution of *N*-stirring under Ar at room temperature. After being stirred for 16 h, the reaction mixture was partitioned between CH₂Cl₂ and H₂O. The organic layer was separated and washed with H₂O, aqueous saturated NaHCO₃ solution, and brine. The solution was dried (Na₂SO₄), filtered, and concentrated to dryness to obtain 0.019 g of (–)-**5l** after silica gel chromatography (EtOAc/hexane, 1:3) and crystallization from hexane/EtOAc. The absolute stereochemistry of (–)-**5l** was determined to be *S* by X-ray crystallography.

2-Fluoro-4-hydroxymethylbenzonitrile (7). 4-Bromo-3-fluorotoluene (**6**, 40.0 g, 0.212 mol) was heated at 90 °C in H₂O (200 mL)-pyridine (200 mL) with mechanical stirring under Ar. Potassium permanganate (KMnO₄) (67 g, 0.424 mol) was added portionwise over 3 h. [Warning: Solid KMnO₄ must be added to the hot reaction mixture.] After 4 h, an HPLC of a filtered sample indicated 50% conversion to the acid. Additional KMnO₄ (50 g) was added portionwise with reaction monitoring by HPLC until > 95% conversion was obtained. The reaction mixture was filtered through Celite, and the filter pad was washed with H₂O, aqueous NaOH, and EtOH. The filtrate was concentrated to a small volume and partitioned between 3 N NaOH solution and diethyl ether. The aqueous basic layer was separated, cooled in an ice-H₂O bath, and acidified slowly with 6 N HCl solution to precipitate 40.8 g (88%) of 4-bromo-3-fluorobenzoic acid as a white solid, mp 190–192 °C. ¹H NMR (CDCl₃): δ 7.83 (dd, 1H, *J* = 2, 9 Hz), 7.78 (dd, 1H, *J* = 2, 8 Hz), 7.67–7.71 (m, 1H).

4-Bromo-3-fluorobenzoic acid (40.8 g, 0.187 mol) was dissolved in THF (250 mL) with magnetic stirring under Ar in an ice-H₂O bath. The cloudy solution was treated dropwise with borane-THF complex (1 M) (374 mL, 0.374 mol) over a 1 h period, maintaining the internal temperature at <10 °C. The reaction mixture was left to warm to room temperature overnight and then cooled in an ice-H₂O bath and treated dropwise with H₂O (150 mL). The THF was removed on a rotary evaporator, and the residue was partitioned between EtOAc and H₂O. The aqueous layer was extracted with EtOAc

(3 × 100 mL), and the organic layers were combined, washed with brine, dried (Na₂SO₄), filtered, and concentrated to give 37.49 g (98%) of 4-bromo-3-fluorobenzyl alcohol as an oil that solidified on standing. ¹H NMR (CDCl₃): δ 7.52 (t, 1H, *J* = 8 Hz), 7.16 (d, 1H, *J* = 9 Hz), 7.02 (d, 1H, *J* = 8 Hz), 4.67 (s, 2H), 1.47 (br s, 1H).

4-Bromo-3-fluorobenzyl alcohol (20 g, 0.097 mol) was dissolved in DMF (100 mL) and then placed under high vacuum for 15 min. The solution was then purged with Ar for 15 min. While purging continued, ZnCN (8 g, 0.068 mol) and the catalyst, Pd[(PPh₃)₄], (5.63 g, 0.0049 mol) were added. The reaction mixture was heated at 95 °C under Ar for 18 h and then cooled to ambient temperature and added to H₂O. The mixture was extracted with EtOAc and then washed with 1 M HCl, H₂O, and brine and dried (Na₂SO₄). Filtration and concentration to dryness gave 11 g (75%) of **7** as a white solid after chromatography (silica gel, 35% EtOAc/hexane). ¹H NMR (CDCl₃): δ 7.61 (t, 1H, *J* = 8 Hz), 7.23–7.29 (m, 2H), 4.80 (d, 2H, *J* = 6 Hz), 1.93 (t, 1H, *J* = 6 Hz).

2-Fluoro-4-imidazol-1-ylmethylbenzotrile (9). Compound **7** (9.06 g, 0.06 mol), CBr₄ (29.76 g, 0.09 mol), and Ph₃P (23.5 g, 0.09 mol) were combined in CH₂Cl₂ (250 mL) [*exothermic reaction*], and the mixture was stirred for 3 h at room temperature. The reaction mixture was concentrated to dryness, and the resulting crude bromide **8**⁸ was added to a solution of imidazole (20.3 g, 0.30 mol) in DMF (250 mL). After the mixture was stirred overnight at room temperature, the DMF was removed in vacuo and the residue was partitioned between EtOAc and H₂O. The organic layer was separated, washed with H₂O (2×), and extracted with 1 N HCl solution. The aqueous acidic layer was separated, neutralized with Na₂CO₃ solution, and extracted with CH₂Cl₂ (3×). The organics were combined and dried (MgSO₄). Filtration and concentration to dryness gave 6.09 g (51%) of **9**. ¹H NMR (CDCl₃): δ 7.62 (dd, 1H, *J* = 8.5, 9.5 Hz), 7.57 (s, 1H), 7.16 (s, 1H), 7.00 (d, 1H, *J* = 8.5 Hz), 6.94 (d, 1H, *J* = 9.5 Hz), 6.91 (s, 1H), 5.21 (s, 2H).

2-Fluoro-4-(1-trityl-1*H*-imidazol-4-ylmethyl)benzotrile (11). Zinc (0.301 g, 4.63 mmol) and dibromoethane (0.040 mL, 0.463 mmol) were stirred in anhydrous THF (2 mL) under Ar for 1.5 h. A solution of **8** (0.546 g, 2.55 mmol) in anhydrous THF (1 mL) was added dropwise, and the mixture was stirred for 1 h. A mixture of 4-iodo-1-trityl-1*H*-imidazole (**10**)¹⁰ (0.808 g, 1.85 mmol) and NiCl₂(PPh₃)₂ (0.120 g, 0.183 mmol) was added. After the mixture was stirred overnight under Ar, the reaction was quenched with saturated NH₄Cl (9 mL) and the mixture was stirred for 2 h. The mixture was extracted with CH₂Cl₂ (3×) and dried (MgSO₄), and the solvents were evaporated. Purification by silica gel chromatography (0.5% MeOH/CH₂Cl₂ with NH₄OH) gave 0.348 g (42%) of **11**.

2-Fluoro-4-formylbenzotrile (12). Compound **7** (10 g, 0.066 mol) and Et₃N (32.3 mL, 0.231 mol) were dissolved in a mixture of 100 mL of CH₂Cl₂ and 20 mL of DMSO. While being stirred, the solution was treated dropwise with a solution of pyridine–SO₃ complex (31.5 g, 0.198 mol) in DMSO (70 mL), maintaining the reaction mixture temperature between 5 and 10 °C. The reaction mixture was stirred at 5 °C for 1 h after the addition and at ambient temperature for 1 h. The reaction mixture was partitioned between CH₂Cl₂ and H₂O. The organic layer was separated, washed well with H₂O and brine, and dried (Na₂SO₄). Filtration and concentration gave 8.9 g (90%) of **12** after purification by chromatography (silica gel, hexane/EtOAc, 3:1). ¹H NMR (CDCl₃): δ 10.06 (d, 1H, *J* = 2 Hz), 7.86 (dd, 1H, *J* = 5, 8 Hz), 7.798 (dd, 1H, *J* = 1, 8 Hz), 7.728 (dd, 1H, *J* = 1, 8 Hz).

2-Fluoro-4-[hydroxy-(1-trityl-1*H*-imidazol-4-yl)methyl]benzotrile (13). To a solution of 4-iodo-1-trityl-1*H*-imidazole (**10**, 5.00 g, 11.5 mmol) in anhydrous CH₂Cl₂ (30 mL) was added a 3.0 M solution of EtMgBr (6.58 mL, 19.7 mmol) with stirring under Ar at room temperature. After 3 h, the reaction mixture was cooled to –78 °C and a solution of **12** (1.73 g, 11.6 mmol) in CH₂Cl₂ (20 mL) was added dropwise. The reaction mixture was allowed to warm to room temperature over 2 h and quenched with saturated NH₄Cl solution. The

pH of the mixture was adjusted to 8.5 with saturated NaHCO₃ solution, and the product was extracted with CH₂Cl₂ (3×). The combined organic layers were dried (MgSO₄), concentrated, and purified by silica gel chromatography (0–1% MeOH/CH₂Cl₂) to yield 5.2 g (98%) of **13**. ¹H NMR (CDCl₃): δ 7.70–7.80 (m, 1H), 7.41 (s, 1H), 7.25–7.38 (m, 1H), 7.05–7.17 (m, 5H), 6.65 (s, 1H), 5.68 (d, 1H, *J* = 7 Hz), 3.36 (d, 1H, *J* = 7 Hz). MS, *m/z*: (M + 1) 460.

Acetic Acid (4-Cyano-3-fluorophenyl)(1-trityl-1*H*-imidazol-4-yl)methyl ester (14). Compound **13** (4.05 g, 8.81 mmol), pyridine (2.14 mL, 26.4 mmol), and Ac₂O (12.5 mL, 132 mmol) were stirred in anhydrous DMF (650 mL) for 3 h under Ar. The reaction mixture was concentrated in vacuo, diluted with EtOAc (250 mL), washed with H₂O (2×) and brine, dried (MgSO₄), and concentrated to give a quantitative yield of **14**, which was used without purification in the subsequent step.

2-Fluoro-4-[hydroxy(1-methyl-1*H*-imidazol-5-yl)methyl]benzotrile (15). Compound **14** (4.60 g, 8.81 mmol) was treated with dimethyl sulfate (0.833 mL, 8.81 mmol) in EtOAc (20 mL) and heated at 60 °C overnight under Ar. The reaction mixture was concentrated in vacuo. The crude imidazolium salt was dissolved in MeOH (30 mL) and refluxed for 1 h. The solution was concentrated in vacuo, and the residue was purified by silica gel chromatography (0.5–4% MeOH/CH₂Cl₂ with NH₄OH) to give 0.838 g (35%) of acetic acid (4-cyano-3-fluorophenyl)(3-methyl-3*H*-imidazol-4-yl)methyl ester. The ester (1.26 g, 4.59 mmol) was treated with NaOH (5.5 mL, 5.5 mmol) in THF (15 mL) and H₂O (25 mL) for 1 h at room temperature. The solution was diluted with saturated aqueous NaHCO₃ solution, extracted with CH₂Cl₂ (3×), dried (MgSO₄), and concentrated to give 0.97 g (91%) of **15**. ¹H NMR (CD₃-OD): δ 7.75 (t, 1H, *J* = 8 Hz), 7.60 (s, 1H), 7.46 (d, 1H, *J* = 10.4 Hz), 7.39 (d, 1H, *J* = 8 Hz), 6.57 (s, 1H), 5.98 (s, 1H), 3.64 (s, 3H).

Alternative Preparation of 15. A solution of 5-lithio-1-methyl-2-(triethylsilyl)-1*H*-imidazole (**17**, 0.199 mol) in THF (500 mL) was prepared at –78 °C as described by Molina.¹¹ The cold solution of **17** was cannulated into a solution of **12** (27.0 g, 0.181 mol) in dry THF (200 mL) over 15 min at –78 °C. The cooling bath was removed, and the mixture was stirred for 2 h while warming to room temperature. After cooling to 0 °C, the reaction mixture was quenched with saturated NH₄Cl solution. The mixture was acidified with 10% HCl, and the THF was removed in vacuo. Solid NaHCO₃ was added to make the mixture basic, and this mixture was extracted with EtOAc (3×). The organic layers were combined, washed with brine, dried (MgSO₄), filtered, and concentrated to dryness to give 28.5 g (68%) of crude **15**, which was used without purification in the preparation of **18**.

2-Fluoro-4-[amino-(1-methyl-1*H*-imidazol-5-yl)methyl]benzotrile (16). Compound **15** (0.542 g, 2.31 mmol) was dissolved in SOCl₂ (15 mL), and the mixture was stirred at room temperature for 2 h under Ar. The solution was concentrated in vacuo and coevaporated three times with CH₂Cl₂. The solid was dissolved in CHCl₃ (30 mL) and cooled to –78 °C. Gaseous NH₃ was bubbled through the solution for 5 min, and the mixture was stirred for 16 h while warming to room temperature under Ar. After concentration to dryness and chromatography (silica gel, 1–2% CH₃OH/CH₂Cl₂ with NH₃), 0.372 g (70%) of **16** was obtained. ¹H NMR (CDCl₃): δ 7.61 (t, 1H, *J* = 7.9 Hz), 7.41 (s, 1H), 7.25–7.30 (m, 2H), 6.86 (s, 1H), 5.27 (s, 1H), 3.52 (s, 3H), 1.70 (br s, 2H). MS, *m/z*: (M + 1) 231.

2-Fluoro-4-(1-methyl-1*H*-imidazole-5-carbonyl)benzotrile (18). Crude alcohol **15** (28.5 g) was dissolved in CH₂Cl₂ (400 mL) and treated with MnO₂ (100 g, 1.15 mol) at room temperature. After 2 h, the reaction mixture was filtered through Celite, and the filter cake was washed with CH₂Cl₂ and CH₃CN. The filtrate was concentrated in vacuo, and the residue was triturated with hexane/EtOAc to give 19.6 g of **18** (45% for two steps). ¹H NMR (CDCl₃): δ 7.77–7.81 (m, 1H), 7.70–7.73 (m, 2H), 7.67 (dd, 1H, *J* = 1.3, 9 Hz), 7.59 (d, 1H, *J* = 1 Hz), 4.03 (s, 3H). MS, *m/z*: (M + 1) 230.

N-[(4-Cyano-3-fluorophenyl)(1-methyl-1*H*-imidazol-5-yl)methylene]-2-methyl-[*S*(*R*)]-propanesulfonamide ((*R*)-19**).** Compound **18** (2.56 g, 11.2 mmol), titanium(IV) ethoxide (7.02 mL, 33.5 mmol), and commercially available (*R*)-(+)-2-methyl-2-propanesulfonamide (1.35 g, 11.2 mmol) were dissolved in anhydrous THF (100 mL) and heated at 75 °C for 7 days. The solution was cooled, diluted with brine (100 mL), and filtered through a Celite pad. The filter cake was washed generously with EtOAc and H₂O. The filtrate was separated, dried (MgSO₄), and purified on silica gel (0–3% MeOH/CH₂-Cl₂) to give 2.94 g (79%) of (*R*)-**19**. ¹H NMR (CDCl₃): δ 7.70–7.76 (m, 1H), 7.67 (s, 1H), 7.25–7.34 (m, 2H), 6.93 (s, 1H), 4.04 (s, 3H), 1.29 (s, 9H). MS, *m/z* (M + 1) 333.

(*S*)-**19** was identically prepared using (*S*)-(–)-2-methyl-2-propanesulfonamide.

(S)-(–) and (R)-(+)-4-[1-Amino-1-(1-methyl-1*H*-imidazol-5-yl)ethyl]-2-fluorobenzonitrile Bishydrochloride ((*S*)-(–) and (*R*)-(+)-20**).** Compound (*R*)-**19** (1.50 g, 4.51 mmol) was dissolved in anhydrous THF (30 mL) at 0 °C, and a 3.0 M solution of MeMgBr (4.50 mL, 13.5 mmol) in Et₂O was added. The reaction was quenched with aqueous NH₄Cl solution, and the mixture was diluted with saturated NaHCO₃ solution and extracted with CH₂Cl₂ (3×). The combined organic layers were dried (MgSO₄), filtered, and concentrated to give 1.57 g (99%) of an 80:20 mixture of 1-((*S*)/(*R*))-*N*-[1-(4-cyano-3-fluorophenyl)-1-(3-methyl-3*H*-imidazol-4-yl)ethyl]-2-methyl-[*S*(*R*)]-propanesulfonamides. Crystallization from 5% hexane in EtOAc gave the 1-(*S*)-[*S*(*R*)] diastereomer (99% pure) as colorless needles, mp 205–207 °C. ¹H NMR (CDCl₃): δ 7.63–7.65 (m, 1H), 7.46 (s, 1H), 7.36 (s, 1H), 7.15–7.17 (m, 2H), 3.75 (s, 1H), 3.08 (s, 3H), 2.08 (s, 3H), 1.28 (s, 9H). Anal. (C₁₇H₂₁N₄OSF·0.35H₂O) C, H, N.

To a solution of this product (0.880 g, 2.51 mmol) in MeOH (50 mL) was added 50 mL of a 4 M HCl solution in dioxane, and the mixture was stirred for 1 h at room temperature. After concentration and trituration with EtOAc, 0.47 g (59%) of (*S*)-(–)-**20** was obtained as the bis HCl salt. [α]_D –111.6° (c 1, EtOH). ¹H NMR (CD₃OD): δ 9.05 (s, 1H), 7.97 (dd, 1H, *J* = 6, 8 Hz), 7.93 (d, 1H, *J* = 1.5 Hz), 7.52 (dd, 1H, *J* = 2, 10 Hz), 7.43 (dd, 1H, *J* = 2, 8 Hz), 3.44 (s, 3H), 2.20 (s, 3H).

Similarly, (*R*)-(+)-**20** ([α]_D +99.6° (c 1, EtOH)) was obtained from (*S*)-**19**. These enantiomeric amines were readily separated on an HPLC Chiracel OD column, eluting with 60:40 EtOH/hexane.

2-[3-(3-Ethyl-1-methyl-2-oxoazepan-3-yl)phenoxy]-4-imidazol-1-ylmethylbenzotriazole Hydrochloride (1**).** Compound **9** (0.045 g, 0.222 mmol), **5c** (0.055 g, 0.222 mmol), KF·Al₂O₃ (0.136 g), and 18-crown-6 (0.006 g, 0.023 mmol) were refluxed in CH₃CN (2.5 mL) under Ar for 48 h (subsequently referred to as standard displacement conditions). The solution was filtered, concentrated in vacuo, and purified using reverse-phase chromatography (95:5 to 5:95 H₂O/CH₃CN with 0.1% TFA, flow = 65 mL/min). The compound was converted to the free base using saturated NaHCO₃ solution, extracted with CH₂Cl₂ (3×), dried (MgSO₄), and filtered. Addition of 1 N HCl in Et₂O gave the hydrochloride salt of racemic **1**. ¹H NMR (CD₃OD): δ 9.01 (s, 1H), 7.83 (d, 1H, *J* = 7.9 Hz), 7.59 (s, 2H), 7.44 (t, 1H, *J* = 7.8 Hz), 7.05 (d, 1H, *J* = 7.5 Hz), 6.99 (d, 1H, *J* = 6.5 Hz), 6.95 (s, 1H), 6.80 (s, 1H), 5.48 (s, 2H), 3.00 (s, 3H), 2.97–3.10 (m, 2H), 2.22–2.27 (m, 1H), 1.71–1.88 (m, 5H), 1.45–1.64 (m, 2H), 0.76 (t, 3H, *J* = 7.1 Hz). MS, *m/z* (M + 1) 429. Anal. (C₂₆H₂₈N₄O₂·1.05HCl·0.05H₂O) C, H, N.

Compound (*S*)-**1** was prepared from (–)-**5c**. [α]_D –22.9° (c 1, EtOH). FAB MS, *m/z* (M + 1) 429. Anal. (C₂₆H₂₈N₄O₂·1.50HCl·1.25H₂O) C, H, N.

Compound (*R*)-**1** was prepared from (+)-**5c**. [α]_D +22.9° (c 1, EtOH). FAB MS, *m/z* (M + 1) 429. Anal. (C₂₆H₂₈N₄O₂·1.00HCl·1.95H₂O) C, H, N.

By use of these standard displacement conditions, compounds **21**, **22**, and **23** were prepared from **5a**, **5i**, and **5j**, respectively.

4-Imidazol-1-ylmethyl-2-[3-(1-methyl-2-oxoazepan-3-yl)phenoxy]benzotriazole Hydrochloride (21**).** ¹H NMR (CD₃OD): δ 9.04 (s, 1H), 7.79 (d, 1H, *J* = 7.7 Hz), 7.62 (s, 1H),

7.56 (s, 1H), 7.39 (t, 1H, *J* = 7.9 Hz), 7.19 (d, 1H, *J* = 7.7 Hz), 7.13 (d, 1H, *J* = 7.3 Hz), 7.03 (s, 1H), 7.00 (d, 1H, *J* = 11 Hz), 5.43 (s, 2H), 4.11 (d, 1H, *J* = 9.1 Hz), 3.85–3.93 (m, 1H), 3.30–3.38 (m, 1H), 3.02 (s, 3H), 1.76–2.07 (m, 5H), 1.52–1.63 (m, 1H). MS, *m/z* (M + 1) 401. Anal. (C₂₄H₂₅N₄O₂·1.00HCl·0.65H₂O·0.20CH₂Cl₂) C, H, N.

4-Imidazol-1-ylmethyl-2-[3-(2-oxoazepan-3-yl)phenoxy]benzotriazole Hydrochloride (22**).** ¹H NMR (CD₃OD): δ 9.02 (s, 1H), 7.78 (d, 1H, *J* = 7.9 Hz), 7.61 (s, 1H), 7.55 (s, 1H), 7.40 (t, 1H, *J* = 8.1 Hz), 7.20 (d, 1H, *J* = 7.8 Hz), 7.15 (d, 1H, *J* = 7.7 Hz), 7.03 (s, 1H), 7.00 (s, 2H), 5.42 (s, 2H), 3.95–4.01 (m, 1H), 3.43–3.51 (m, 1H), 3.24–3.33 (m, 1H), 1.78–2.10 (m, 5H), 1.45–1.58 (m, 1H). MS, *m/z* (M + 1) 387. Anal. (C₂₃H₂₂N₄O₂·1.00HCl·0.40CH₂Cl₂) C, H, N.

2-[3-(3-Ethyl-2-oxoazepan-3-yl)phenoxy]-4-imidazol-1-ylmethylbenzotriazole (23**).** ¹H NMR (CD₃OD): δ 8.98 (s, 1H), 7.82 (d, 1H, *J* = 7.9 Hz), 7.58 (s, 2H), 7.47 (t, 1H, *J* = 7.9 Hz), 7.22 (d, 1H, *J* = 9 Hz), 7.15 (d, 1H, *J* = 7.8 Hz), 7.01 (dd, 1H, *J* = 2.4, 8.1 Hz), 6.93 (s, 1H), 6.91 (s, 1H), 5.46 (s, 2H), 2.88–2.95 (m, 1H), 2.60–2.70 (m, 1H), 2.24–2.31 (m, 1H), 1.71–1.96 (m, 5H), 1.59–1.67 (m, 1H), 1.37–1.48 (m, 1H), 0.78 (t, 3H, *J* = 7.3 Hz). MS, *m/z* (M + 1) 415. Anal. (C₂₅H₂₆N₄O₂·1.00HCl·0.10H₂O·0.40CH₂Cl₂) C, H, N.

2-[3-(3-Ethyl-azepan-3-yl)phenoxy]-4-imidazol-1-ylmethylbenzotriazole Bishydrochloride (24**).** Compounds **9** (0.113 g, 0.560 mmol) and **5k** (0.123 g, 0.560 mmol) were reacted under standard displacement conditions to give 0.045 g (16%) of compound **24**. ¹H NMR (CD₃OD): δ 9.03 (s, 1H), 7.83 (d, 1H, *J* = 7.9 Hz), 7.61 (s, 1H), 7.58 (s, 1H), 7.51 (t, 1H, *J* = 8 Hz), 7.30 (d, 1H, *J* = 7.9 Hz), 7.19–7.22 (m, 2H), 7.08 (s, 1H), 7.01 (dd, 1H, *J* = 2, 8 Hz), 5.50 (s, 2H), 3.80 (d, 1H, *J* = 14.5 Hz), 3.36 (d, 1H, *J* = 14.5 Hz), 3.12–3.35 (m, 2H), 2.35–2.44 (m, 1H), 1.83–1.98 (m, 4H), 1.68–1.81 (m, 3H), 0.66 (t, 3H, *J* = 7.5 Hz). MS, *m/z* (M + 1) 401. Anal. (C₂₅H₂₈N₄O₁·2.00HCl·0.10H₂O·0.45CH₂Cl₂) C, H, N.

2-[3-(1-Acetyl-3-ethylazepan-3-yl)phenoxy]-4-imidazol-1-ylmethylbenzotriazole Hydrochloride (25**).** Compound **24** (0.116 g, 0.184 mmol), Et₃N (0.103 mL, 0.736 mmol), and acetyl chloride (0.020 mL, 0.276 mmol) were dissolved in anhydrous CH₂Cl₂ (5 mL). After 1 h, the reaction mixture was concentrated in vacuo and purified using reverse-phase chromatography (95:5 to 5:95 H₂O/CH₃CN with 0.1% TFA, flow = 65 mL/min). The compound was converted to its free base using saturated NaHCO₃ solution, extracted with CH₂Cl₂ (3×), dried (MgSO₄), filtered, and treated with 1 N HCl ethereal solution to give 0.036 g (41%) of compound **25**. ¹H NMR (CD₃OD): δ 9.00 (s, 1H), 7.81 (d, 1H, *J* = 8 Hz), 7.60 (s, 1H), 7.57 (s, 1H), 7.40 (t, 1H, *J* = 7.9 Hz), 7.28 (d, 1H, *J* = 8.2 Hz), 7.19 (d, 1H, *J* = 8 Hz), 6.93–6.96 (m, 2H), 5.45 (s, 2H), 3.92 (d, 1H, *J* = 14.2 Hz), 3.73 (d, 1H, *J* = 14.2 Hz), 3.55–3.72 (m, 1H), 2.10–2.20 (m, 1H), 2.07 (s, 3H), 1.65–1.87 (m, 8H), 0.57 (t, 3H, *J* = 7.4 Hz). MS, *m/z* (M + 1) 443. Anal. (C₂₇H₃₀N₄O₂·1.00HCl·0.35H₂O·0.40CH₂Cl₂) C, H, N.

2-[3-(3-Ethyl-1-methyl-2-oxoazepan-3-yl)phenoxy]-4-(1*H*-imidazol-5-ylmethyl)benzotriazole Hydrochloride (27**).** Compounds **11** (0.348 g, 0.784 mmol) and **5c** (0.194 mg, 0.784 mmol) were reacted under standard displacement conditions to give 0.30 g (57%) of 2-[3-(3-ethyl-1-methyl-2-oxoazepan-3-yl)phenoxy]-4-(1-trityl-1*H*-imidazol-4-ylmethyl)benzotriazole (**26**). Without purification, **26** (0.074 g, 0.110 mmol) was treated with TFA (2.5 mL) and Et₃SiH (0.140 mL, 0.882 mmol) in CH₂-Cl₂ (5 mL) at room temperature for 1 h. The solvent was evaporated and the residue was purified by reverse-phase chromatography (95:5 to 5:95 H₂O/CH₃CN with 0.1% TFA, flow = 65 mL/min) to give 0.024 g (47%) of **27**. ¹H NMR (CD₃OD): δ 8.83 (s, 1H), 7.75 (d, 1H, *J* = 7.8 Hz), 7.43 (t, 1H, *J* = 7.6 Hz), 7.32 (s, 1H), 7.18 (d, 1H, *J* = 7.9 Hz), 7.04 (d, 1H, *J* = 7.7 Hz), 6.98 (d, 1H, *J* = 7.2 Hz), 6.85 (s, 1H), 6.76 (s, 1H), 4.12 (s, 2H), 2.99 (s, 3H), 2.92–3.11 (m, 2H), 2.20–2.29 (m, 1H), 1.65–1.92 (m, 5H), 1.40–1.65 (m, 2H), 0.74 (t, 3H, *J* = 7.1 Hz). MS, *m/z* (M + 1) 429. Anal. (C₂₆H₂₉N₄O₂·1.00HCl·0.10H₂O·0.35CH₂-Cl₂) C, H, N.

2-[3-(3-Ethyl-1-methyl-2-oxoazepan-3-yl)phenoxy]-4-(1-methyl-1*H*-imidazol-5-ylmethyl)benzotriazole Hydrochloride

ride (28). Dimethyl sulfate (0.014 mL, 0.149 mmol) and **26** (0.100 g, 0.149 mmol) were dissolved in EtOAc (10 mL) and heated at 60 °C for 18 h under Ar. The reaction mixture was concentrated in vacuo, triturated with Et₂O, dissolved in MeOH (15 mL), and refluxed for 1 h. The solution was concentrated in vacuo and purified using reverse-phase chromatography (95:5 to 5:95 H₂O/CH₃CN with 0.1% TFA, flow = 65 mL/min). The compound was converted to its free base using saturated NaHCO₃ solution, extracted with CH₂Cl₂ (3×), dried (MgSO₄), filtered, and treated with 1 N HCl ethereal solution to give 0.030 g (42%) of **28**. ¹H NMR (CD₃OD): δ 8.86 (s, 1H), 7.77 (d, 1H, *J* = 7.7 Hz), 7.44 (t, 1H, *J* = 7.9 Hz), 7.23 (s, 1H), 7.18 (d, 1H, *J* = 7.7 Hz), 7.04 (d, 1H, *J* = 7.5 Hz), 6.99 (d, 1H, *J* = 7.0 Hz), 6.88 (s, 1H), 6.76 (s, 1H), 4.15 (s, 2H), 3.73 (s, 3H), 2.99 (s, 3H), 2.95–3.11 (m, 2H), 2.20–2.29 (m, 1H), 1.65–1.91 (m, 5H), 1.44–1.62 (m, 2H), 0.74 (t, 3H, *J* = 7.1 Hz). MS, *m/z*: (M + 1) 443. HRMS calcd for C₂₇H₃₀N₄O₂ (M + 1)⁺: 443.2442, found 443.2431.

2-[3-(3-Ethyl-1-methyl-2-oxoazepan-3-yl)phenoxy]-4-[hydroxy-(1-methyl-1*H*-imidazol-5-yl)methyl]benzotriazole (29). Compounds **15** (0.162 g, 0.700 mmol) and **5c** (0.173 g, 0.700 mmol) were reacted under standard displacement conditions to give 0.118 g (36%) of compound **29**. ¹H NMR (CD₃OD): δ 7.74 (d, 1H, *J* = 8 Hz), 7.55 (s, 1H), 7.44 (t, 1H, *J* = 8 Hz), 7.24 (d, 1H, 8 Hz), 7.00–7.05 (m, 3H), 6.83–6.84 (m, 1H), 6.51 (d, 1H, *J* = 7.1 Hz), 5.86 (s, 1H), 3.58 (d, 3H, *J* = 3.3 Hz), 2.99 (d, 3H, *J* = 4 Hz), 2.90–3.08 (m, 2H), 2.20–2.28 (m, 1H), 1.68–1.89 (m, 5H), 1.51–1.60 (m, 1H), 1.40–1.50 (m, 1H), 0.74 (t, 3H, *J* = 7.3 Hz). MS, *m/z*: (M + 1) 459. Anal. (C₂₇H₃₀N₄O₃·0.30CH₂Cl₂) C, H, N.

4-[Amino-(1-methyl-1*H*-imidazol-5-yl)methyl]-2-[3-(3-ethyl-1-methyl-2-oxoazepan-3-yl)phenoxy]benzotriazole (30). Compound **29** (0.093 g, 0.202 mmol) was dissolved in SOCl₂ (5 mL), and the mixture was stirred at room temperature for 2 h under Ar. The solution was concentrated in vacuo and coevaporated with CH₂Cl₂ (3×). The solid was dissolved in CHCl₃ (20 mL), and the solution was cooled to –78 °C. NH₃(g) was bubbled through the solution, and the solution was stirred for 16 h while warming to room temperature under Ar. The solution was concentrated in vacuo and purified using reverse-phase chromatography (95:5 to 5:95 H₂O/CH₃CN with 0.1% TFA, flow = 65 mL/min). The compound was converted to its free base using saturated NaHCO₃ solution, extracted with CH₂Cl₂ (3×), dried (MgSO₄), filtered, and concentrated to give 0.031 g (34%) of **30**. ¹H NMR (CDCl₃): δ 7.63 (t, 1H, *J* = 7.7 Hz), 7.34–7.40 (m, 2H), 7.06–7.16 (m, 1H), 6.97–7.04 (m, 1H), 6.78–6.96 (m, 3H), 6.73 (s, 1H), 5.10 (s, 1H), 3.47 (s, 3H), 3.03 (s, 3H), 3.02–3.10 (m, 1H), 2.82–2.90 (m, 1H), 2.13–2.22 (m, 1H), 1.67–1.95 (m, 7H), 1.53–1.62 (m, 1H), 1.39–1.51 (m, 1H), 0.75 (t, 3H, *J* = 7.1 Hz). MS, *m/z*: (M + 1) 458. Anal. (C₂₇H₃₁N₅O₂·0.35H₂O) C, H, N.

2-[3-(3-Ethyl-1-methyl-2-oxoazepan-3-yl)phenoxy]-4-(1-methyl-1*H*-imidazole-5-carbonyl)benzotriazole Trifluoroacetate (31). Compounds **16** (0.012 g, 0.052 mmol) and **5c** (0.014 g, 0.056 mmol) were reacted under standard displacement conditions to give 0.010 g (33%) of compound **31**, which was isolated as the TFA salt after reverse-phase HPLC. ¹H NMR (CD₃OD): δ 8.85 (s, 1H), 8.00 (s, 1H), 7.97 (d, 1H, *J* = 8 Hz), 7.70 (dd, 1H, *J* = 2, 8 Hz), 7.50 (t, 1H, *J* = 8 Hz), 7.31 (s, 1H), 7.06–7.13 (m, 2H), 6.92 (s, 1H), 4.09 (s, 3H), 3.01 (s, 3H), 2.97–3.13 (m, 2H), 2.23–2.32 (m, 1H), 1.70–1.94 (m, 5H), 1.42–1.69 (m, 2H), 0.76 (t, 3H, *J* = 7.3 Hz). MS, *m/z*: (M + 1) 457. HRMS calcd for C₂₇H₂₈N₄O₃ (M + 1)⁺: 457.2234, found 457.2232.

2-[3-(3-Ethyl-1-methyl-2-oxoazepan-3-yl)phenoxy]-4-[1-hydroxy-1-(1-methyl-1*H*-imidazol-5-yl)ethyl]benzotriazole (32). To a solution of **31** (0.216 g, 0.473 mmol) in anhydrous THF (10 mL) was added a 3.0 M solution of MeMgBr (1.10 mL, 3.30 mmol) with stirring at room temperature. The reaction was quenched with NH₄Cl after 1 h and the mixture was concentrated, diluted with EtOAc, washed with saturated NaHCO₃ solution, water, and brine, dried (MgSO₄), concentrated, and purified by silica gel chromatography (1–3% MeOH/CH₂Cl₂ with NH₄OH) to give 0.125 g

(56%) of **32**. ¹H NMR (CDCl₃): δ 7.57 (d, 1H, *J* = 8 Hz), 7.36 (t, 1H, *J* = 7.8 Hz), 7.32 (s, 1H), 6.90–7.07 (m, 5H), 6.78 (s, 1H), 3.24 (s, 3H), 3.02 (s, 3H), 3.04–3.10 (m, 1H), 2.83–2.90 (m, 1H), 2.41–2.51 (m, 1H), 2.12–2.20 (m, 1H), 1.82 (s, 3H), 1.60–1.93 (m, 6H), 1.38–1.50 (m, 1H), 0.74 (t, 3H, *J* = 7.2 Hz). HRMS calcd for C₂₈H₃₂N₄O₃ (M + 1)⁺: 473.2553, found 473.2600.

Mixture of Diastereomers of 2-[3-(3-Ethyl-1-methyl-2-oxoazepan-3-yl)phenoxy]-4-[1-amino-1-(1-methyl-1*H*-imidazol-5-yl)ethyl]benzotriazole (33). Compound **32** (0.099 g, 0.209 mmol) was dissolved in SOCl₂ (5 mL), and the mixture was stirred at room temperature for 2 h. The solution was concentrated in vacuo and coevaporated with anhydrous CH₂Cl₂ (3×). The solid was dissolved in CHCl₃ (5 mL) and cooled to –78 °C. NH₃(g) was bubbled through the solution, and the mixture was stirred for 2 h while warming to room temperature under Ar. The solution was concentrated in vacuo and purified using reverse-phase chromatography (95:5 to 5:95 H₂O/CH₃CN with 0.1% TFA, flow = 65 mL/min). The compound was converted to its free base using saturated NaHCO₃ solution, extracted with CH₂Cl₂ (3×), dried (MgSO₄), and filtered to give 0.052 g (52%) of **33**. ¹H NMR (CD₃OD): δ 7.72 (d, 1H, *J* = 7.9 Hz), 7.48 (s, 1H), 7.40 (t, 1H, *J* = 8.1 Hz), 7.22–7.28 (m, 1H), 6.96–7.03 (m, 2H), 6.92 (d, 1H, *J* = 8 Hz), 6.89 (s, 1H), 6.74–6.78 (m, 1H), 3.25 (s, 3H), 2.99 (s, 3H), 2.92–3.08 (m, 2H), 2.18–2.27 (m, 1H), 1.66–1.89 (m, 5H), 1.73 (s, 3H), 1.55–1.65 (m, 1H), 1.40–1.53 (m, 1H), 0.74 (t, 3H, *J* = 7.3 Hz). MS, *m/z*: (M + 1) 472. Anal. (C₂₈H₃₃N₅O₂·0.35EtOAc) C, H, N.

All four diastereomers of **33** were independently prepared using the standard displacement conditions described for compound **1** using the resolved intermediates **5c** and **20**.

(*S*)-(–)-**5c** and (*S*)-(–)-**20** gave **33a**. ¹H NMR (CD₃OD): δ 7.72 (d, 1H, *J* = 8 Hz), 7.52 (s, 1H), 7.40 (t, 1H, *J* = 8 Hz), 7.24 (dd, 1H, *J* = 1.5, 8 Hz), 6.98–7.01 (m, 2H), 6.93 (dd, 1H, *J* = 2, 8 Hz), 6.89 (d, 1H, *J* = 1.5 Hz), 6.77 (s, 1H), 3.26 (s, 3H), 2.99 (s, 3H), 2.92–3.08 (m, 2H), 2.21–2.27 (m, 1H), 1.66–1.89 (m, 5H), 1.73 (s, 3H), 1.55–1.65 (m, 1H), 1.40–1.53 (m, 1H), 0.74 (t, 3H, *J* = 7.3 Hz). MS, *m/z*: (M + 1) 472. Anal. (C₂₈H₃₃N₅O₂·0.70H₂O) C, H, N.

(*R*)-(+)-**5c** and (*S*)-(–)-**20** gave **33b**. ¹H NMR (CD₃OD): δ 7.72 (d, 1H, *J* = 8 Hz), 7.48 (s, 1H), 7.40 (t, 1H, *J* = 8 Hz), 7.25 (dd, 1H, *J* = 1.5, 8 Hz), 6.99–7.01 (m, 2H), 6.93 (dd, 1H, *J* = 2, 8 Hz), 6.89 (d, 1H, *J* = 1.5 Hz), 6.75 (t, 1H, *J* = 2 Hz), 3.25 (s, 3H), 2.99 (s, 3H), 2.92–3.08 (m, 2H), 2.21–2.27 (m, 1H), 1.66–1.89 (m, 5H), 1.73 (s, 3H), 1.55–1.65 (m, 1H), 1.40–1.53 (m, 1H), 0.74 (t, 3H, *J* = 7.3 Hz). MS, *m/z*: (M + 1) 472. Anal. (C₂₈H₃₃N₅O₂) C, H, N.

(*S*)-(–)-**5c** and (*R*)-(+)-**20** gave **33c**. ¹H NMR (CD₃OD): δ 7.72 (d, 1H, *J* = 8 Hz), 7.52 (s, 1H), 7.40 (t, 1H, *J* = 8 Hz), 7.24 (dd, 1H, *J* = 1.5, 8 Hz), 6.98–7.01 (m, 2H), 6.93 (dd, 1H, *J* = 2, 8 Hz), 6.89 (d, 1H, *J* = 1.5 Hz), 6.77 (s, 1H), 3.26 (s, 3H), 2.99 (s, 3H), 2.92–3.08 (m, 2H), 2.21–2.27 (m, 1H), 1.66–1.89 (m, 5H), 1.73 (s, 3H), 1.55–1.65 (m, 1H), 1.40–1.53 (m, 1H), 0.74 (t, 3H, *J* = 7.3 Hz). MS, *m/z*: (M + 1) 472. Anal. (C₂₈H₃₃N₅O₂·0.70H₂O·0.25H₂O) C, H, N.

(*R*)-(+)-**5c** and (*R*)-(+)-**20** gave **33d**. ¹H NMR (CD₃OD): δ 7.72 (d, 1H, *J* = 8 Hz), 7.49 (s, 1H), 7.40 (t, 1H, *J* = 8 Hz), 7.24 (dd, 1H, *J* = 1.5, 8 Hz), 6.98–7.01 (m, 2H), 6.93 (dd, 1H, *J* = 2, 8 Hz), 6.88 (d, 1H, *J* = 1.5 Hz), 6.77 (t, 1H, *J* = 2 Hz), 3.25 (s, 3H), 2.99 (s, 3H), 2.92–3.08 (m, 2H), 2.21–2.27 (m, 1H), 1.66–1.89 (m, 5H), 1.73 (s, 3H), 1.55–1.65 (m, 1H), 1.40–1.53 (m, 1H), 0.74 (t, 3H, *J* = 7.3 Hz). MS, *m/z*: (M + 1) 472. Anal. (C₂₈H₃₃N₅O₂·0.65H₂O) C, H, N.

Except for compound **34**, the final compounds listed in Table 4 were prepared by the standard displacement reaction of (*S*)-(–)-**20** with the requisite phenol (–)-**5**. Compound **34** was obtained from (*S*)-(–)-**20** and racemic **5b**. Note that the assignment of the absolute configuration¹⁴ of compounds **5** (except for **5c**) was not rigorously determined but inferred to be analogous to **5c** based on their common levorotatory nature, their consistent relative retention time upon chiral-phase HPLC, and the rank order of enzyme inhibitory potency of the diastereomers of **34**–**40** (data not shown).

2-[3-(1-Methyl-2-oxoazepan-3(*R,S*)-yl)phenoxy]-4-[1(*S*)-amino-1-(1-methyl-1*H*-imidazol-5-yl)ethyl]benzotrifluoroacetate (34). ¹H NMR (CD₃OD): δ 8.47 (d, 1H, *J* = 8 Hz), 7.86 (t, 1H, *J* = 8 Hz), 7.55–7.60 (m, 1H), 7.40 (q, 1H, *J* = 8 Hz), 7.01–7.18 (m, 5H), 4.09–4.14 (m, 1H), 3.86–3.95 (m, 1H), 3.35–3.45 (m, 1H), 3.37 (d, 3H, *J* = 9 Hz), 3.00 (d, 3H, *J* = 10.5 Hz), 2.01 (d, 3H, *J* = 13.5 Hz), 1.80–2.00 (m, 5H), 1.49–1.62 (m, 1H). MS, *m/z* (M + 1) 444. Anal. (C₂₆H₃₁N₅O₂·2.15CF₃CO₂H·0.25H₂O) C, H, N.

2-[3-(1,3-Dimethyl-2-oxoazepan-3(*S*)-yl)phenoxy]-4-[1(*S*)-amino-1-(1-methyl-1*H*-imidazol-5-yl)ethyl]benzotrifluoroacetate (35). ¹H NMR (CD₃OD): δ 8.53 (s, 1H), 7.88 (d, 1H, *J* = 8.2 Hz), 7.55 (s, 1H), 7.46 (t, 1H, *J* = 8 Hz), 7.26 (dd, 1H, *J* = 1.6, 8 Hz), 7.09 (d, 1H, *J* = 7.7 Hz), 7.02 (d, 1H, *J* = 1.5 Hz), 6.99 (dd, 1H, *J* = 1.6, 8 Hz), 6.79 (s, 1H), 3.42 (s, 3H), 3.02 (s, 3H), 2.97–3.06 (m, 2H), 2.27–2.34 (m, 1H), 1.97 (s, 3H), 1.75–1.89 (m, 3H), 1.58–1.68 (m, 1H), 1.42–1.53 (m, 1H), 1.34 (s, 3H). HRMS calcd for C₂₇H₃₁N₅O₂ (M + 1)⁺: 458.2551, found 458.2576.

2-[3-(3(*S*)-Propyl-1-methyl-2-oxoazepan-3-yl)phenoxy]-4-[1(*S*)-amino-1-(1-methyl-1*H*-imidazol-5-yl)ethyl]benzotrifluoroacetate (36). ¹H NMR (CD₃OD): δ 8.56 (s, 1H), 7.86 (d, 1H, *J* = 8 Hz), 7.57 (d, 1H, *J* = 1.3 Hz), 7.44 (t, 1H, *J* = 8 Hz), 7.22 (dd, 1H, *J* = 1.7, 8 Hz), 7.09 (d, 1H, *J* = 1.6 Hz), 7.07 (d, 1H, *J* = 7.7 Hz), 6.97 (dd, 1H, *J* = 2.4, 8 Hz), 6.78 (t, 1H, *J* = 2 Hz), 3.44 (s, 3H), 3.00 (s, 3H), 2.96–3.10 (m, 2H), 2.24–3.02 (m, 1H), 1.97 (s, 3H), 1.84–1.949 (m, 2H), 1.64–1.78 (m, 3H), 1.46–1.64 (m, 2H), 1.20–1.33 (m, 1H), 1.05–1.16 (m, 1H), 0.82 (t, 3H, *J* = 7.3 Hz). HRMS calcd for C₂₇H₃₁N₅O₂ (M + 1)⁺: 486.2864, found 486.2870.

2-[3-(3(*R*)-Cyclopropylmethyl-1-methyl-2-oxoazepan-3-yl)phenoxy]-4-[1(*S*)-amino-1-(1-methyl-1*H*-imidazol-5-yl)ethyl]benzotrifluoroacetate (37). ¹H NMR (CD₃OD): δ 7.72 (d, 1H, *J* = 8 Hz), 7.49 (s, 1H), 7.38 (t, 1H, *J* = 8 Hz), 7.25 (dd, 1H, *J* = 1.6, 8 Hz), 7.03 (d, 1H, *J* = 8 Hz), 6.98 (d, 1H, *J* = 1.3 Hz), 6.91–6.94 (m, 2H), 6.81 (t, 1H, *J* = 2 Hz), 3.26 (s, 3H), 3.01 (s, 3H), 2.92–3.07 (m, 2H), 2.39–2.46 (m, 1H), 1.97 (s, 3H), 1.84–1.95 (m, 2H), 1.73 (s, 3H), 1.68–1.83 (m, 2H), 1.55–1.67 (m, 2H), 1.40–1.53 (m, 1H), 0.67–0.78 (m, 1H), 0.17–0.31 (m, 1H), –0.18 to –0.26 (m, 1H), –0.29 to –0.36 (m, 1H). MS, *m/z* (M + 1) 498. Anal. (C₃₀H₃₅N₅O₂·0.40H₂O) C, H, N.

2-[3-(1-Methyl-2-oxo-3-(*R*)-(3,3,3-trifluoropropyl)azepan-3-yl)phenoxy]-4-[1(*S*)-amino-1-(1-methyl-1*H*-imidazol-5-yl)ethyl]benzotrifluoroacetate (38). ¹H NMR (CD₃OD): δ 7.75 (d, 1H, *J* = 8 Hz), 7.66 (s, 1H), 7.46 (t, 1H, *J* = 8 Hz), 7.22 (dd, 1H, *J* = 1.6, 8 Hz), 7.09 (s, 1H), 7.05 (d, 1H, *J* = 7.5 Hz), 6.96–7.09 (m, 2H), 6.83 (s, 1H), 3.30 (s, 3H), 3.01 (s, 3H), 2.96–3.09 (m, 2H), 2.24–2.36 (m, 2H), 1.99–2.08 (m, 1H), 1.74–1.94 (m, 5H), 1.77 (s, 3H), 1.58–1.66 (m, 1H), 1.41–1.53 (m, 1H). MS, *m/z* (M + 1) 540. Anal. (C₂₉H₃₂N₅O₂F₂·0.65H₂O) C, H, N.

2-[3-(3(*S*)-*n*-Butyl-1-methyl-2-oxoazepan-3-yl)phenoxy]-4-[1(*S*)-amino-1-(1-methyl-1*H*-imidazol-5-yl)ethyl]benzotrifluoroacetate (39). ¹H NMR (CD₃OD): δ 8.61 (s, 1H), 7.88 (d, 1H, *J* = 8 Hz), 7.60 (d, 1H, *J* = 1.53 Hz), 7.43 (t, 1H, *J* = 8 Hz), 7.24 (dd, 1H, *J* = 1.7, 8 Hz), 7.12 (d, 1H, *J* = 1.7 Hz), 7.06 (d, 1H, *J* = 8.6 Hz), 6.95 (dd, 1H, *J* = 1.6, 7.5 Hz), 6.79 (t, 1H, *J* = 2 Hz), 3.44 (s, 3H), 3.00 (s, 3H), 2.96–3.09 (m, 2H), 2.23–3.00 (m, 1H), 1.98 (s, 3H), 1.82–1.96 (m, 2H), 1.67–1.77 (m, 3H), 1.47–1.62 (m, 2H), 1.17–1.27 (m, 3H), 1.07–1.17 (m, 1H), 0.84 (t, 3H, *J* = 7.3 Hz). MS, *m/z* (M + 1) 500. Anal. (C₃₀H₃₅N₅O₂·2.50CF₃CO₂H·1.0H₂O) C, H, N.

2-[3-(3(*R*)-Cyclopropylethyl-1-methyl-2-oxoazepan-3-yl)phenoxy]-4-[1(*S*)-amino-1-(1-methyl-1*H*-imidazol-5-yl)ethyl]benzotrifluoroacetate (40). ¹H NMR (CD₃OD): δ 8.55 (s, 1H), 7.86 (d, 1H, *J* = 8 Hz), 7.57 (d, 1H, *J* = 1.1 Hz), 7.43 (t, 1H, *J* = 8 Hz), 7.22 (dd, 1H, *J* = 1.8, 8 Hz), 7.11 (d, 1H, *J* = 1.8 Hz), 7.06 (d, 1H, *J* = 8 Hz), 6.95 (dd, 1H, *J* = 2.3, 7.5 Hz), 6.78 (t, 1H, *J* = 1.8 Hz), 3.44 (s, 3H), 2.99 (s, 3H), 2.90–3.09 (m, 2H), 2.21–2.28 (m, 1H), 1.97 (s, 3H), 1.78–1.93 (m, 4H), 1.68–1.78 (m, 1H), 1.43–1.62 (m, 2H), 1.12–1.22 (m, 1H), 0.95–1.05 (m, 1H), 0.49–0.59 (m, 1H), 0.30–0.37 (m, 2H), –0.05 to 0.05 (m, 2H), –0.04 to –0.10 (m, 2H). HRMS calcd for C₃₁H₃₉N₅O₂ (M + 1)⁺: 512.3020, found 512.2991.

Table 5. Data and Refinement Statistics: HFTase + FPP + **33a**

resolution, Å	37–2.0
total reflections	278 618
unique reflections	75 205
<i>R</i> _{sym} , %	7.8 (34.1) ^a
average <i>I</i> /σ	14.4 (2.3) ^a
completeness <i>F</i> > 0σ(<i>F</i>), %	94.7 (82.4) ^a
<i>R</i> _{work} , %	17.9
<i>R</i> _{free} , %	20.8
number of residues	710
number of solvent molecules	690
average <i>B</i> factor, Å ²	21.9
rmsd bond angle, deg	1.17
rmsd bond length, Å	0.006

^a Highest resolution bin.

Inhibition Assays. Inhibition of FTase is reported as an IC₅₀, the concentration of compound required to inhibit 50% of the recombinant human FTase-catalyzed incorporation of [³H]FPP into recombinant Ras-CVIM (a fusion protein that consists of part yeast Ras1 sequence and part human Ras sequence with the CaaX box of K-Ras). For details of the method, see refs 19 and 20.

For GGTase-I, the IC₅₀ is the concentration of compound required to inhibit 50% of the human GGTase-I-catalyzed incorporation of [³H]GGPP into a biotinylated peptide corresponding to the C-terminus of human K-Ras. For the qualitative determination of competition between inhibitors and geranylgeranyl pyrophosphate (GGPP), IC₅₀ values were determined at 20, 100, and 500 nM GGPP. The following slopes of the plots of IC₅₀ vs [GGPP] were observed: **33a**, –0.09; **35**, –0.28; **36**, –0.19; **37**, –0.03; **38**, –0.09; **39**, –0.19. Slopes of <0 indicate that binding is not competitive with GGPP and are consistent with uncompetitive binding. Details of these assays are found in ref 17.

Cell-Based Assays. To determine the potential of these compounds to exhibit dual FTase/GGTase-I inhibition in vivo and to consequently inhibit the prenylation of K-Ras, selected compounds were tested in PSN-1 pancreatic tumor cells as described by Lobell et al.¹⁸ Briefly, tumor cells were treated for 24 h with inhibitors. The cell lysates were subjected to SDS-PAGE and Western blot using antibodies specific for hDJ2, Rap1a, or K-Ras. Unprocessed and prenylated proteins were distinguished by virtue of their different electrophoretic mobilities.

Animal Studies. As described in detail in ref 18, nude mice bearing PSN-1 tumor xenografts were treated with compounds **33a** and **38** by constant infusion for 24–72 h using implanted Alzet osmotic pumps. Doses ranged from 240 to 1920 mpk/day, which afforded plasma levels of 2–15 μM.

Crystallography Methods. Human farnesyltransferase was concentrated to 10 mg/mL and combined with FPP and inhibitor dissolved in 25 mM DMSO in a 1:3:1.5 molar ratio. Diffraction quality crystals were grown using the hanging drop vapor diffusion method from a mother liquor of 200–400 mM ammonium acetate and 12–14% PEG 8K, pH 5.3–5.5, at 17 °C. Diffraction data were collected at cryogenic temperature using an *R*-axis IV image plate (Molecular Structure Corporation) mounted on a Rigaku RU-200 rotating anode X-ray source with double mirror optics. Data were reduced using DENZO and SCALEPACK.²¹ The space group of the crystals was determined to be *P*6₁ with cell dimensions *a* = *b* = 178.4 Å and *c* = 64.6 Å. Phases were obtained by molecular replacement with human farnesyltransferase, PDB accession number 1JCQ.²² Model building proceeded using the program O,²³ and the coordinates were refined using the program CNS.²⁴ Diffraction data and final refinement statistics are summarized in Table 5. Coordinates have been deposited in the Protein Data Bank with accession number 1MZC.

Supporting Information Available: Details from the crystallographic structure determination of **5l**. This material is available free of charge via the Internet at <http://pubs.acs.org>.

References

- (1) Rodenhuis, S. Ras and human tumors. *Semin. Cancer Biol.* **1992**, *3*, 241–247.
- (2) For a recent review, see the following. Bell, I. M. Inhibitors of Protein Prenylation. *Expert Opin. Ther. Pat.* **2000**, *10*, 1813–1821.
- (3) Cox, A. D.; Der, C. J. Farnesyltransferase Inhibitors and Cancer Treatment: Targeting Simply Ras. *Biochim. Biophys. Acta* **1997**, *1333*, F51–F71.
- (4) Sun, J.; Qian, Y.; Hamilton, A. D.; Sebti, S. M. Both Farnesyltransferase and Geranylgeranyltransferase I Inhibitors Are Required for Inhibition of Oncogenic K-Ras Prenylation but Each Alone Is Sufficient To Suppress Human Tumor Growth in Nude Mouse Xenografts. *Oncogene* **1998**, *16*, 1467–1473.
- (5) Rowell, C. A.; Kowalczyk, J. J.; Lewis, M. D.; Garcia, A. M. Direct Demonstration of Geranylgeranylation and Farnesylation of Ki-Ras In Vivo. *J. Biol. Chem.* **1997**, *272*, 14092–14097.
- (6) MacTough, S. C.; deSolms, S. J.; Shaw, A. W.; Abrams, M. T.; Ciccarone, T. M.; Davide, J. P.; Hamilton, K. A.; Hutchinson, J. H.; Koblan, K. S.; Kohl, N. E.; Lobell, R. B.; Robinson, R. G.; Graham, S. L. Diaryl Ether Inhibitors of Protein-Farnesyltransferase. *Bioorg. Med. Chem. Lett.* **2001**, *11*, 1257–1260.
- (7) White, A. C.; Bradley, G.; Cavalla, J. F.; Edington, T.; Shepherd, R. G.; Bushell, B. J.; Johnson, J. R.; Weston, G. O. Synthetic studies on meptazinol. Anion chemistry in the synthesis of α -aryl lactams. *Eur. J. Med. Chem.* **1980**, *15*, 375–385.
- (8) Hutchinson, J. H.; deSolms, S. J.; Graham, S. L.; Shaw, A. W.; Ciccarone, T. M. Inhibitors of Prenyl-Protein Transferase. Patent WO9917777, April 15, 1999.
- (9) Lee, K.; Jung, W.-H.; Hwang, S. Y.; Lee, S.-H. Fluorobenzamidozation thrombin inhibitors: influence of fluorine on enhancing oral absorption. *Bioorg. Med. Chem. Lett.* **1999**, *9*, 2483–2486.
- (10) Jetter, M. C.; Boyd, R. E.; Reitz, A. B. Expedient synthesis of N1-tritylimidazole-4-carboxaldehyde. *Org. Prep. Proced. Int.* **1996**, *28*, 709–710.
- (11) Molina, P.; Fresneda, P. M.; Garciazafrá, S. Iminophosphorane-mediated synthesis of 1-acyl- β -carboline: a new access to the alkaloids eudistomin T, S and xestomanzamine A of marine origin. *Tetrahedron Lett.* **1996**, *37*, 9353–9356.
- (12) Cogan, D. A.; Liu, G.; Ellman, J. A. Asymmetric synthesis of chiral amines by highly diastereoselective 1,2-additions of organometallic reagents to *N*-*tert*-butanesulfinyl imines. *Tetrahedron* **1999**, *55*, 8883–8904.
- (13) Shaw, A. W.; deSolms, S. J. Asymmetric synthesis of α,α -diaryl and α -aryl- α -heteroaryl alkylamines by organometallic additions to *N*-*tert*-butanesulfinyl ketimines. *Tetrahedron Lett.* **2001**, *42*, 7173–7176.
- (14) Levorotatory phenols have the azepinone 3(*S*) stereochemistry except **5e**, **5f**, and **5h** where the priority rules confer the 3(*R*) designation.
- (15) Long, S. B.; Hancock, P. J.; Kral, A. M.; Hellinga, H. W.; Beese, L. S. The Crystal Structure of Human Protein Farnesyltransferase Reveals the Basis for Inhibition by CaaX Tetrapeptides and Their Mimetics. *Proc. Nat. Acad. Sci. U.S.A.* **2001**, *98*, 12948–12953.
- (16) Anthony, N. J.; Gomez, R. P.; Schaber, M. D.; Mosser, S. D.; Hamilton, K. A.; O'Neil, T. J.; Koblan, K. S.; Graham, S. L.; Hartman, G. D.; Shah, D.; Rands, E.; Kohl, N. E.; Gibbs, J. B.; Oliff, A. I. Design and in Vivo Analysis of Potent Non-Thiol Inhibitors of Farnesyl Protein Transferase. *J. Med. Chem.* **1999**, *42*, 3356–3368.
- (17) Huber, H. E.; Robinson, R. G.; Watkins, A.; Nahas, D. D.; Abrams, M. T.; Buser, C. A.; Lobell, R. B.; Patrick, D.; Anthony, N. J.; Dinsmore, C. J.; Graham, S. L.; Hartman, G. D.; Lumma, W. C.; Williams, T. M.; Heimbrook, D. C. Anions Modulate the Potency of Geranylgeranyl-Protein Transferase I Inhibitors. *J. Biol. Chem.* **2001**, *276*, 24457–24465.
- (18) Lobell, R. B.; Omer, C. A.; Abrams, M. T.; Bhimnathwala, H. G.; Brucker, M. J.; Buser, C. A.; Davide, J. P.; deSolms, S. J.; Dinsmore, C. J.; Ellis-Hutchings, M. S.; Kral, A. M.; Liu, D.; Lumma, W. C.; Machotka, S. V.; Rands, E.; Williams, T. M.; Graham, S. L.; Hartman, G. D.; Heimbrook, D. C.; Kohl, N. E. Evaluation of Farnesyl:Protein Transferase and Geranylgeranyl-Protein Transferase Inhibitor Combinations in Preclinical Models. *Cancer Res.* **2001**, *61*, 8758–8768.
- (19) Moores, S. L.; Schaber, M. D.; Mosser, S. D.; Rands, E.; O'Hara, M. B.; Garsky, V. M.; Marshall, M. S.; Pompliano, D. L.; Gibbs, J. B. Sequence-Dependence of Protein Isoprenylation. *J. Biol. Chem.* **1991**, *266*, 14603–14610.
- (20) Omer, C. A.; Kral, A. M.; Diehl, R. A.; Prendergast, G. C.; Powers, S.; Allen, C. M.; Gibbs, J. B.; Kohl, N. E. Characterization of Recombinant Human Farnesyl-Protein Transferase: Cloning, Expression, Farnesyl Diphosphate Binding and Functional Homology with Yeast Prenyl-Protein Transferases. *Biochemistry* **1993**, *32*, 5167–5176.
- (21) Otwinowski, Z.; Minor, W. *Methods in Enzymology, Macromolecular Crystallography (Part A): Processing of X-ray Diffraction Data Collected in Oscillation Mode*; Academic Press: New York, 1997.
- (22) Long, S. B.; Hancock, P. J.; Kral, A. M.; Hellinga, H. W.; Beese, L. S. The Crystal Structure of Human Protein Farnesyltransferase Reveals the Structural Basis for Inhibition by CaaX Tetrapeptides and Their Mimetics. *Proc. Natl. Acad. Sci. U.S.A.* **2001**, *98*, 12948–12953.
- (23) Jones, T. A.; Kjeldgaard, M. *O*, version 5.9 (and the manual); Uppsala University: Uppsala, Sweden, 1993.
- (24) Brunger, A. T.; Adams, P. D.; Clore, G. M.; DeLano, W. L.; Gros, P.; Grosse-Kunstleve, R. W.; Jiang, J. S.; Kuszewski, J.; Nilges, M.; Pannu, N. S.; Read, R. J.; Rice, L. M.; Simonson, T.; Warren, G. L. Crystallography & NMR System: A New Software Suite for Macromolecular Structure Determination. *Acta Crystallogr., Sect. D* **1998**, *D54*, 905–921.

JM020587N